37. Kim,J.H., Stansbury,K.H., Walker,N.J., Trush,M.A., Strickland,P.T. and Sutter,T.R. (1998) Metabolism of benzo[*a*]pyrene and benzo[*a*]pyrene-7,8-diol by human cytochrome P450 1B1. *Carcinogenesis*, 19, 1847–1853.
38. Shimada,T., Oda,Y., Gillam,E.M., Guengerich,F.P. and Inoue,K. (2001) Metabolic activation of polycyclic aromatic hydrocarbons and other procarcinogens by cytochromes P450 1A1 and P450 1B1 allelic variants and other human cytochromes P450 in *Salmonella typhimurium* NM2009. *Drug Metab. Dispos.*, 29, 1176–1182.
39. Buetler,T.M., Gallagher,E.P., Wang,C., Stahl,D.L., Hayes,J.D. and Eaton,D.L. (1995) Induction of phase I and phase II drug-metabolizing enzyme mRNA, protein and activity by BHA, ethoxyquin and oltipraz. *Toxicol. Appl. Pharmacol.*, 135, 45–57.
40. Murray,G.I. (2000) The role of cytochrome P450 in tumour development and progression and its potential in therapy. *J. Pathol.*, 192, 419–426.
41. Dey,A., Jones,J.E. and Nebert,D.W. (1999) Tissue- and cell type-specific expression of cytochrome P450 1A1 and cytochrome P450 1A2 mRNA in the mouse localized *in situ* hybridization. *Biochem. Pharmacol.*, 58, 525–537.
42. Thapliyal,R., Deshpande,S.S. and Maru,G.B. (2002) Mechanism(s) of turmeric-mediated protective effects against benzo(a)pyrene-derived DNA adducts. *Cancer Lett.*, 175, 79–88.
43. Ryu,D.Y. and Hodgson,E. (1999) Constitutive expression and induction of CYP1B1 mRNA in the mouse. *J. Biochem. Mol. Toxicol.*, 13, 249–251.
44. Shimada,T., Inoue,K., Suzuki,Y. *et al.* (2002) Arylhydrocarbon receptor-dependent induction of liver and lung cytochromes P450 1A1, 1A2 and 1B1 by polycyclic aromatic hydrocarbons and polychlorinated biphenyls in genetically engineered C57BL/6J mice. *Carcinogenesis*, 23, 1199–1207.
45. Kensler,T.W., Groopman,J.D., Sutter,T.R., Curphey,T.J. and Roebuck,B.D. (1999) Development of cancer chemopreventive agents: oltipraz as a paradigm. *Chem. Res. Toxicol.*, 12, 113–126

Received October 16, 2002; revised November 25, 2002; accepted November 26, 2002

THE JOURNAL OF BIOLOGICAL CHEMISTRY
Vol. 278, No. 10, Issue of March 7, pp. 8135–8145, 2003
Printed in U.S.A.

Modulation of Gene Expression by Cancer Chemopreventive Dithiolethiones through the Keap1-Nrf2 Pathway

IDENTIFICATION OF NOVEL GENE CLUSTERS FOR CELL SURVIVAL*

Received for publication, November 21, 2002, and in revised form, December 18, 2002
Published, JBC Papers in Press, December 27, 2002, DOI 10.1074/jbc.M211898200

Mi-Kyoung Kwak‡, Nobunao Wakabayashi‡§, Ken Itoh§, Hozumi Motohashi§, Masayuki Yamamoto§, and Thomas W. Kensler‡¶

From the ‡Department of Environmental Health Sciences, Johns Hopkins University Bloomberg School of Public Health, Baltimore, Maryland 21205 and the §Institute of Basic Medical Sciences and Center for Tsukuba Advanced Research Alliance, University of Tsukuba, Tennoudai, Tsukuba 305-8577, Japan

Enzyme inducers such as 3*H*-1,2-dithiole-3-thione (D3T) enhance the detoxication of environmental carcinogens and protect against neoplasia. The putative molecular sensor for inducers is Keap1, a sulfhydryl-rich protein that sequesters the transcription factor Nrf2 in the cytoplasm. Expression of these detoxication enzymes is blunted in *nrf2*-deficient mice; moreover, these mice are more sensitive to carcinogenesis, and the protective actions of dithiolethiones are lost with *nrf2* disruption. Hepatic gene expression profiles were examined by oligonucleotide microarray analysis in vehicle- or D3T-treated wild-type mice as well as in *nrf2* single and *keap1-nrf2* double knockout mice to identify those genes regulated by the Keap1-Nrf2 pathway. Transcript levels of 292 genes were elevated in wild-type mice 24 h after treatment with D3T; 79% of these genes were induced in wild-type, but not *nrf2*-deficient mice. These *nrf2*-dependent, D3T-inducible genes included known detoxication and antioxidative enzymes. Unexpected clusters included genes for chaperones, protein trafficking, ubiquitin/26 S proteasome subunits, and signaling molecules. Gene expression patterns in *keap1-nrf2* double knockout mice were similar to those in *nrf2*-single knockout mice. D3T also led to *nrf2*-dependent repression of 31 genes at 24 h; principally genes related to cholesterol/lipid biosynthesis. Collectively, D3T increases the expression of genes through the Keap1-Nrf2 signaling pathway that directly detoxify toxins and generate essential cofactors such as glutathione and reducing equivalents. Induction of *nrf2*-dependent genes involved in the recognition and repair/removal of damaged proteins expands the role of this pathway beyond primary control of electrophilic and oxidative stresses into secondary protective actions that enhance cell survival.

Inducers of phase 2 and antioxidative enzymes are known to enhance the detoxication of environmental carcinogens in animals, often leading to protection against neoplasia (1, 2). Use of enzyme inducers as cancer chemopreventive agents in humans is currently under clinical investigation (3, 4). Regulation of both basal and inducible expression of cytoprotective genes is mediated in part by the antioxidant response element (ARE),[1] a cis-acting sequence found in the 5′-flanking region of genes encoding many phase 2 enzymes including mouse glutathione *S*-transferase (GST) A1, human NAD(P)H quinone oxidoreductase (NQO1), and human γ-glutamylcysteine ligase as well as murine Nrf2 itself (5–8). Recently, Maf and CNC-bZIP ("cap"n collar family of basic region leucine zipper proteins) transcription factors such as Nrf2 have been shown to be ARE-binding proteins (9, 10). Overexpression of Nrf2 in human hepatoma cells enhanced both basal and inducible activation of an ARE reporter gene (10). Increased nuclear accumulation of Nrf2 has been observed in the liver of mice treated with 3H-1,2-dithiole-3-thione (D3T), a potent chemopreventive agent (8, 11). Initially, this accumulation results from translocation of Nrf2 from the cytoplasm. Itoh *et al.* (12) have identified and characterized Keap1, an actin-binding protein localized to the cytoplasm that sequesters Nrf2 by specific binding to its N-terminal regulatory domain (13). Administration of sulfhydryl reactive compounds, such as diethylmaleate or D3T, abolishes Keap1 repression of Nrf2 activity in cells and facilitates the nuclear accumulation of Nrf2 (14, 15). Recently, Dinkova-Kostova *et al.* (16) has shown in a cell-free system that selective cysteine amino acids in Keap1 can react directly with a sulfhydryl reactive inducer, dexamethasone mesylate, and trigger the release of Nrf2 from Keap1. These results support the hypothesis that Keap1 is a key regulatory molecule of Nrf2 and that the Keap1-Nrf2 complex acts as a sensor to oxidative or electrophilic stresses to induce protective genes promoting cell survival.

Studies with *nrf2*-disrupted mice indicated that Nrf2 was essential for the induction of GST and NQO1 activities *in vivo* by different classes of chemopreventive agents including dithiolethiones, isothiocyanates, and phenolic antioxidants (9, 11, 17). A series of studies from several laboratories have been undertaken over the past decade to better understand the range of genes coordinately induced by these agents so as to elucidate the biochemical basis for protection. Genes now recognized as induced through the Nrf2-ARE signaling system include a panel of xenobiotic conjugating enzymes, enzymes that provide cofactors and

* This work was supported by Grants CA39416 and CA94076 from the National Institutes of Health and Center Grant ES 03819. The costs of publication of this article were defrayed in part by the payment of page charges. This article must therefore be hereby marked "*advertisement*" in accordance with 18 U.S.C. Section 1734 solely to indicate this fact.

¶ To whom correspondence should be addressed: Dept. of Environmental Health Sciences, Johns Hopkins University Bloomberg School of Public Health, 615 N. Wolfe St., Baltimore, MD 21205. Tel.: 410-955-4712; Fax: 410-955-0116; E-mail: tkensler@jhsph.edu.

[1] The abbreviations used are: ARE, antioxidant response element; D3T, 3*H*-1,2-dithiole-3-thione; GST, glutathione *S*-transferase; NQO1, NAD(P)H:quinone oxidoreductase; mEH, microsomal epoxide hydrolase; NFκB, nuclear factor κB; Hsp, heat shock protein; CV, coefficients of variation; AFC, average fold change; RT-PCR, reverse transcriptase-polymerase chain reaction.

reducing equivalents for these reactions, and antioxidative enzymes and proteins (11, 17–20). Collectively, these gene products facilitate the detoxication and elimination of toxic electrophilic and free radical metabolites of xenobiotics. The likely importance of these protective enzymes is highlighted by recent observations that *nrf2*-knockout mice were considerably more sensitive to the acute toxicities of acetaminophen, butylated hydroxytoluene, and hyperoxia (21–24). These mice also form higher levels of DNA adducts following exposure to carcinogens such as aflatoxin B_1, diesel particulate matter, and benzo[a]pyrene (25–27). Moreover, *nrf2*-disrupted mice are substantially more sensitive to the tumorigenicity of benzo[a]pyrene (28).

Dithiolethiones such as D3T, anethole dithiolethione, and oltipraz inhibit the toxicity and carcinogenicity of many chemical carcinogens in multiple target organs (29–32) and are undergoing preclinical and clinical evaluations for use as cancer chemopreventive agents. Interestingly, the chemoprotective efficacy of dithiolethiones and other enzyme inducers is lost in *nrf2*-knockout mice (28). Gene-disrupted animals provide elegant models for assessing the molecular mechanisms underlying the pharmacodynamic actions of chemopreventive agents. In this study, we have used *nrf2*-knockout mice and *keap1-nrf2* double knockout mice to probe the role of the Keap1-Nrf2-ARE signaling pathway in protecting cells against stress conditions. Through the use of oligonucleotide array technology it is apparent that not only are primary defense systems involving detoxication enzymes induced through this pathway, but that secondary defense mechanisms involving surveillance and repair of damaged biomolecules are also activated.

EXPERIMENTAL PROCEDURES

Animals and Treatments—Wild-type and *nrf2*-disrupted mice were generated from inbred *nrf2* heterozygous mice (9, 11). *Keap1-nrf2* double knockout mice were generated by mating *nrf2* −/− mice with *keap1* +/− mice to obtain the double homozygous mice (33). Genotypes were determined by PCR using primers TGGACGGGACTATTGAAGGCTG, GCCGCCTTTTCAGTAGATGGAGG, and GCGGATTGACCGTAATGGGATAGG for *nrf2*, and CGGGATCCCCATGGAAAGGCTTATTGAGTTC, GAAGTGCATGTAGATATACTCCC, and TCAGAGCAGCCGATTGTCTGTTGTGCCCAGTCA for *keap1*. For the microarray analyses three male mice were used per group. Mice were fed AIN-76A semipurified diet for at least 10 days before treatment. 10–12-week-old mice were treated with 0.5 mmol/kg of D3T by gavage in a suspension consisting of 1% Cremophor and 25% of glycerol. Mice were sacrificed 6 h or 24 h after treatment, and livers were removed and snap-frozen. Additional mice were fed basal AIN-76A diet or diet supplemented with 0.03% (w/w) D3T for 7 days and sacrificed at day 8. The selected doses of D3T are the respective maximum tolerated doses for gavage and chronic dietary administration and do not affect body weight or other clinical signs over longer periods. It is estimated that the dietary dose provided about half of the amount of D3T per day that was administered in the single oral dose. *Keap1-nrf2* double knockout mice were treated with either vehicle or D3T (0.5 mmol/kg) by gavage and sacrificed 24 h after treatment for microarray analysis of hepatic gene expression.

Sample Preparation for Microarray Analysis—Total RNA was isolated from frozen liver using the Totally RNA kit (Ambion, Austin, TX). Isolated RNA was then purified using the RNeasy Mini kit (Qiagen, Valencia, CA). cDNA was synthesized from total RNA using the Superscript Choice kit (Invitrogen, Carlsbad, CA) with a T7-$(dT)_{24}$ primer. Biotin-labeled cRNA was prepared from cDNA by *in vitro* transcription (Enzo Biochemical, Farmingdale, NY) and fragmented by incubation at 94 °C for 45 min in 40 mM Tris acetate buffer, pH 8.1, with 100 mM potassium and 30 mM magnesium acetate.

Hybridization and Scanning—Fragmented cRNA (12.5 μg) was hybridized at 45 °C for 16 h to a Murine Genome U74Av2 GeneChip® (Affymetrix, Santa Clara, CA) containing probes for ~12,400 genes and expressed sequence tags (ESTs). Genechips were washed and stained using a fluid station and scanned using an Affymetrix Genechip system confocal scanner.

Data Analysis—Affymetrix Microarray Suite 4.1 was used for expression analysis and fluorescence intensity was measured for each probe array and normalized to the average fluorescence intensity for the entire probe array. Pairwise comparison between data from individual mice (n = 3), generating 9 comparisons, was performed. The change in gene expression for each gene was calculated as a ratio of average $\text{difference}_{(\text{D3T-treated})}$/average $\text{difference}_{(\text{vehicle-treated})}$ and average fold changes from nine comparisons were obtained. To evaluate the reproducibility of paired comparisons, coefficients of variation (CV, S.D./mean) for the average difference change was applied, and 1.0 was used as a cutoff value (34). After evaluating reproducibility, genes having comparison numbers of ≥7 were selected to filter out the false positive responses. Genespring software (Silicon Genetics, San Carlos, CA) and the Affymetrix Analysis Center website were used for the annotation of genes. For analysis of the distributions of gene families, expression levels of each gene category were plotted as histograms as described by Bouton and Pevsner (35).

RT-PCR Analysis—RT-PCR was performed on genes induced or repressed by D3T to confirm the microarray results. For the synthesis of cDNAs, 50 ng of total RNA was incubated for 20 min with 10 mM Tris (pH 8.4), 5 mM KCl, 5 mM $MgCl_2$, 4 mM dNTPs, 0.125 μg of oligo$(dT)_{12-18}$ and 30 units of M-MRV (Moloney Murine Leukemia Virus) reverse transcriptase (Invitrogen). PCR amplification for each gene was performed with a Fail Safe PCR kit (Epicentere, Madison, WI) using a DNA thermal cycler (MJ Research, Watertown, MA). Amplification conditions were 26–29 cycles for 5 min at 95 °C, 30 s at 56 °C and 40 s at 72 °C. PCR primers specific to NQO1, mEH, and albumin were used as described previously (11). Other primers were synthesized by Integrated DNA Technology (Coralville, IA) and were as follows: GST Mu3 (GenBank™ accession number J03953) CAAGTTATGGACACCCGCAT and AGGCACTTGGGCTCAAACAT; UDP-glucose dehydrogenase (X06358) GACATGAATGACTACCAGAG and GTACGGAATTCTCTTGGAAG; heat shock protein 40 homolog b11 (AW122551) TACGATGATATCACTTCCTC and GGCGAGATTTCTATAAGATC; p58 (U28423) GTACGATGAAGCCATTCAGG and CCTTGCCATGAGTTCCAACT; proteasome subunit beta type 3 (AW045339) TTCAGCGTCCTGGTGGTGAT and ACAGAGCCTGTCATTGCTGG; 26 S proteasome-associated pad 1 homolog (Y13071); TATCAACACTCAGCAGAGCT and AATCCTTCCATCCAACTCT; 26 S proteasome ATPase 3 (AA409481) CCCTCAGACCACGGA and TGTGTGAGCGGGTATGAT; mCAR2 (AF009328) TTGTGCAGTTCAAGCCTCCAG and GCGTCCTCCATCTTGTAGCAA; carbonic anhydrase 3 (AJ006474) AACAGGAGCAAGAAAGAG and AGGTCTTCCCATTGTTCA. PCR products were electrophoresed on 1.8% agarose gels and the gel image captured and quantified with a VersaDoc Imaging System (BioRad).

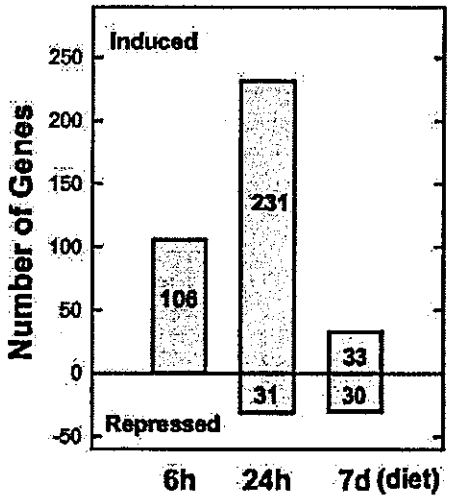

FIG. 1. **Modulation of Nrf2-dependent gene expression by D3T in mouse liver.** Hepatic gene expression patterns were analyzed 6 or 24 h after a single administration of D3T and following addition of D3T to the diet for 7 days. The number of genes increased or decreased only in wild-type mice, not in *nrf2*-knockout mice, are indicated for each group.

RESULTS

D3T-altered Gene Expression in Mouse Liver—Oligonucleotide microarray was used to analyze the gene expression profiles in mouse liver following D3T treatment with a primary

goal of identifying those genes that are regulated through the Keap1/Nrf2 signaling pathway. Expression levels of 352 genes (2.84% of the total genes on the array) were changed in the liver of wild-type mice 24 h after treatment with the potent chemoprotective agent D3T. 129 and 292 genes were increased 6 and 24 h after D3T treatment, respectively, while only 34 were elevated after feeding D3T for 1 week. Most of the D3T-induced genes were dependent on Nrf2 as 82, 79, and 97% of D3T-inducible genes were increased in wild-type mice but not in *nrf2*-disrupted mice in the 6 h, 24 h, and dietary treatment groups, respectively (Fig. 1). A much smaller number of genes were down-regulated by D3T (60 genes at 24 h). Also shown in Fig. 1, D3T suppressed the expression of 31 genes 24 h after treatment and 30 genes following dietary administration in wild-type mice only. Expression of most of these Nrf2-dependent, D3T-modulated genes was not altered in the *keap1-nrf2* double knockout mice 24 h after treatment with D3T. Only 15 out of the 231 Nrf2-dependent, D3T-inducible genes and 2 of the Nrf2-dependent, D3T-repressed genes were affected by D3T in these double knockout mice. Thus, D3T treatment altered the expression of only a modest subset of genes in the liver of wild-type mice and most of these genes were regulated through the Keap1/Nrf2 pathway. Comparisons of expression patterns at different time points indicated that maximal changes occurred 24 h after a single administration of D3T.

Nrf2-dependent, D3T-inducible Genes at 24 h—Genes up-regulated by D3T in wild-type, but not *nrf2*-disrupted mice, were regarded as Nrf2-dependent, D3T-inducible genes. The 231 Nrf2-dependent genes elevated 24 h after treatment with D3T can be classified in several functional categories including xenobiotic metabolizing enzymes, antioxidants, chaperone/stress response proteins, ubiquitin/proteasome systems, acute response/immunity proteins, cytoskeletal organization proteins, protein trafficking proteins, membrane transport proteins, signaling molecules, transcription factors and regulators, and RNA processing/translation-related factors (Table I). As expected from earlier studies, a substantial number (26) of genes related to xenobiotic metabolism were induced by D3T treatment in a *nrf2*-dependent manner. This gene category includes seven genes belonging to cytochrome P450 subfamilies. Ten genes related to glutathione synthesis and conjugation were induced by D3T only in wild-type mice and those included seven subunits of GSTs, glutathione reductase, and the regulatory and catalytic subunits of γ-glutamylcysteine ligase. NQO1, mEH, and UDP-glucuronosyl transferase 2 were also induced. Flavin-containing monooxygenase-1, carbonyl reductase and aldo-keto reductase family 1 were previously unrecognized D3T-inducible genes in mouse liver regulated through Nrf2. These results confirmed our previous observations that xenobiotic detoxifying genes are a major category of genes affected by D3T and *nrf2* genotype. Several antioxidative genes were also induced by D3T; thioredoxin, thioredoxin reductase, and peroxiredoxin transcripts were increased by 2.2-, 3.2-, and 1.7-fold, respectively, 24 h after treatment. General enzymes including nucleotide diphosphatase (3.9-fold), aldolase 1A (2.2-fold), and amino levulinate synthase 1 (3.9-fold) were increased only in wild-type mice. UDP-glucose dehydrogenase was increased by D3T only in wild-type mice 6 h after treatment and in both genotypes 24 h after treatment; however, the induction in wild-type (7.5-fold) was much higher than in *nrf2*-disrupted (1.7-fold) mice.

Twenty genes related to proteasomes as well as genes involved in ubiquitination (ubiquitin-conjugating enzymes E2-32, Huntington-interacting protein-2 and valosin-containing protein) were identified as Nrf2-dependent, D3T-induced genes. The average fold changes of these proteasome subunits ranged from 1.8 to 3.5. Five additional proteasome subunits (proteasome subunit alpha types 2, 5, and 7; delta type 4; and ATPase subunit 2) were induced in both wild-type and *nrf2*-disrupted mice, but with a higher AFC in the wild-type mice (AFC of wild-type/knockout, subunit alpha 2, 2.5/1.4; alpha 5, 2.9/1.6; alpha 7, 2.7/1.4; delta 4, 3.5/1.8; and subunit ATPase 2, 2.9/1.5). Further, proteasome subunit delta 4 was induced equally by D3T in wild-type and *nrf2*-knockout mice. Therefore, in the aggregate, induction of 25 proteasome subunit genes by D3T was affected by *nrf2* genotype.

Other major categories of genes induced by D3T through a Nrf2 pathway were chaperone-protein trafficking systems. These included heat shock proteins, ClpP protease, peptidylproryly isomerase B, and FK506-binding protein 5, which are involved in the repair of unfolded/misfolded proteins as well as genes for protein transport across the endoplasmic reticulum such as the vesicle docking proteins and Sec61. Acute response and inflammatory proteins such as serum amyloids and CD8b and cytoskeletal organization/binding proteins including profilin 2 and protein 4.1 were increased by D3T in wild-type mouse liver. Signaling molecules affected by D3T included NFκB essential modulator, protein inhibitor of nitric-oxide synthase and GTP-binding proteins (ARF-1, Ran, and Gna11). Some genes related to transcription were also categorized as Nrf2-dependent, D3T-induced genes in mice liver. The transcription factor ATF4 family ATF7 was increased 3.6-fold and CRE/ATF family protein X-box-binding protein 1 was increased 2.1-fold by D3T in wild-type mice only. Nuclear receptor mCAR2, transcription activator COP9 subunit 5, and tumor rejection antigen gp96 were also elevated. Lastly, genes affecting mRNA stability/processing-related (small nuclear RNA and poly(rC)-binding protein) and translation (eIF3-p44 and eIF2a) were induced by D3T.

Nrf2-dependent Genes at Other Time Points—Transcripts for 106 genes were increased by D3T 6 h after treatment and remained elevated for 54 of these genes 24 h after treatment. Many genes related to xenobiotic metabolism were substantially induced severalfold or more by 6 h, *e.g.* Cyp2a4 (12.4-fold), NQO1 (5.2-fold), and γ-glutamylcysteine ligase catalytic subunit (3.6-fold), and remained elevated at 24 h. Redox-regulating molecules such as thioredoxin and thioredoxin reductase also showed rapid induction. Expression of half of the rapidly induced genes returned to basal levels at 24 h after treatment. Crystalline αC (2.0-fold), aldehyde oxidase 1 (2.9-fold), anti-apoptotic Bag3 (2.5-fold), mATF4 (1.7-fold), and gelsolin (2.5-fold) were increased only 6 h after treatment by D3T in an Nrf2-dependent manner.

Gene expression profiling was also examined following feeding D3T for 7 days for comparison to that of single administration of D3T. Expression levels of most genes, which were induced by single administration of D3T, returned to basal levels despite continuous administration of D3T in the diet for 7 days. Transcripts for 34 genes remained elevated in this group, 33 of which were for Nrf2-dependent genes. Among the xenobiotic metabolizing enzymes, only two genes (*Cyp3a13* and *Cyp4a10*) were sustainably elevated by D3T in the diet and transcripts for other genes such as NQO1 and the GSTs were not induced over this longer time period. Similarly, no proteasome subunits were detected as D3T-inducible genes with D3T in the diet for 7 days. Deoxyribonuclease IIα, GRO1 oncogene, ICAM-1, and cytokine inducible SH2-containing protein 3 exhibited large increases in this exposure group. D3T in the diet for 7 days also repressed the expression of 30 genes in an Nrf2-dependent manner. Genes repressed at 24 h as well as this later time point included carbonic anhydrase 3, sterol regulatory element-binding protein 1, and Spot 14.

TABLE I
Hepatic Keap1-Nrf2-dependent, D3T-inducible genes

Categories of genes	Accession no.	Description of genes	AFC (D3T/vehicle)			
			WT[a]			*nrf2-keap1*[b] *double KO*
			6 h	*24 h*	*Diet (7 days)*	*24 h*
Chaperone system/stress response genes	U27830	Stress-induced phosphoprotein 1		2.04		
	M18186	Heat shock protein, 84 kDa 1		2.22		
	Z97207	Butyrate-induced transcript 1		2.43		
	AW122551	Hsp40 homolog, subfamily B, member 11		4.14		
	AI835630	Hsp40 homolog, subfamily B, member 9			1.97	
	J04633	Hsp, 86 kD 1		4.11		
	U28423	p58		5.21		
	AI835981	Similar to cisplatin-resistance related protein		2.17		
	AI835644	Endoplasmic reticulum protein 29		1.96		
	AJ005253	ClpP protease		1.97		
	Z31399	η subunit of the chaperonin containing TCP-1		1.92		
	X58990	Peptidylprolyl isomerase B		2.00		
	U16959	FK506-binding protein 5		4.56		2.77
	AI848798	Crystallin, α C	2.04			
	AI846938	Homocysteine-inducible, endoplasmic reticulum Stress-inducible, ubiquitin-like domain member 1			1.51	
Ubiquitin-proteasome	AI836804	Psma1, proteasome α-subunit 1		2.17		
	AJ851441	Psma4, proteasome α-subunit 4		2.16		
	AW048997	Psma5, proteasome α-subunit 5	1.34			
	AW121552	Psma6, proteasome α-subunit 6		1.80		
	AI836676	Psma7, proteasome α-subunit 7		2.71		
	U60824	Psmb1, proteasome β-subunit 1		1.87		
	AI853269	Psmb2, proteasome β-subunit 2		2.17		
	AW045339	Psmb3, proteasome β-subunit 3		2.91		
	U65636	Psmb4, proteasome β-subunit 4		2.28		
	AB003304	Psmb5, proteasome β-subunit 5		2.85		
	UI3393	Psmb6, proteasome β-subunit 6		2.23		
	U39302	Psmc1, proteasome subunit, ATPase 1		2.39		
	AA409481	Psmc3, proteasome subunit, ATPase 3		2.01		
	AW123318	Psmd1, proteasome subunit, nonATPase 1		2.90		
	AI835520	Psmd5, proteasome subunit nonATPase 5		3.11		
	M64641	Psmd7, proteasome subunit nonATPase 7		2.03		
	AW121693	Psmd11, proteasome subunit nonATPase 11	1.51	2.35		
	AI838669	Psmd12, proteasome subunit nonATPase 12		3.25		
	AW045451	Psmd13, proteasome subunit nonATPase 13		2.11		
	Y13071	26 S proteasome-associated pad1 homolog		3.51		
	D49686	Tat-binding protein-1		2.93		
	AW120683	Ubiquitin-conjugating enzyme E2–32		2.91		
	AI836406	Ubiquitin 2	1.85	2.93		
	AW060186	Ubiquitin-specific protease 14	2.17			
	X51703	Ubiquitin b	1.41			
	AB011081	Huntingtin-interacting protein-2		2.53		
	Z14044	Murine valosin-containing protein	1.30	2.50		
Xenobiotic-metabolizing enzymes	X04283	Cyp1a2	1.34			
	M19319	Cyp2a4	12.38			
	L06463	Cyp2a12		2.41		
	X63023	Cyp3a13			1.80	
	AB018421	Cyp4a10			2.51	
	Y11638	Cyp4a14		5.66		9.45
	AF047726	Cyp2c39	4.47			3.89
	U12961	NAD(P)H menadione oxidoreductase (NQO1)	5.24	5.98		
	J03952	Glutathione *S*-transferase, mu 1	1.45	3.07		
	J04696	Glutathione *S*-transferase, mu 2		4.41		
	J03953	Glutathione *S*-transferase, mu 3	1.74	4.63		
	L06047	Glutathione *S*-transferase, alpha 4	1.39	3.25		
	J03958	Glutathione *S*-transferase, alpha 2	2.17	5.86		
	X98056	Glutathione *S*-transferase, theta 2		3.32		1.84
	AI843448	Microsomal glutathione *S*-transferase 3	1.52			
	U85414	γ-glutamylcysteine synthetase, catalytic	3.63	2.83		
	U95053	γ-glutamylcysteine synthetase, regulatory	1.56	2.36		
	U89491	Microsomal epoxide hydrolase	2.73	4.03		2.69
	X06358	UDP-glucuronosyltransferase 2 family, member 5	1.40	1.88		
	D16215	Flavin-containing monooxygenase 1	1.63	2.62		
	U31966	Carbonyl reductase	1.51	5.94		
	AI839814	Aldo-keto reductase family 1, member A1		1.84		
	AB017482	Aldehyde oxidase 1	2.89			
Antioxidant	AI851983	Glutathione reductase 1	1.57	4.50		
	AI118194	Peroxiredoxin 1		1.66		
	AB023564	Type 1 peroxiredoxin		1.69		
	X77585	Thioredoxin	1.28	2.16	1.22	
	AB027565	Thioredoxin reductase 1	2.67	3.18		

TABLE I—*continued*

Categories of genes	Accession no.	Description of genes	AFC (D3T/vehicle)			
			WT[a]			*nrf2-keap1*[b] *double KO*
			6 h	*24 h*	*Diet (7 days)*	*24 h*
General enzymes	AF061017	UDP-glucose dehydrogenase	3.78			
	J02652	Malate oxidoreductase	1.96			
	Y00516	Aldolase 1, A isoform	1.61	2.19		
	AF033381	Betaine homocysteine methyl transferase		1.92		
	M73329	Phospholipase C-α		3.32		
	U51805	Arginase		2.22		
	M28666	Porphobilinogen deaminase		2.01		
	U18975	β-1, 4 *N*-acetylgalactosaminyltransferase		1.77		
	K01515	Hypoxanthine phosphoribosyltransferase		1.88		
	AF118128	Nuclear RNA helicase Bat1		1.96		
	AI846600	Monoglyceride lipase		1.74		
	L31777	Triosephosphate isomerase		1.79		
	M63245	Amino levulinate synthase 1	1.57	3.94		3.43
	AW124201	1-acylglycerol-3-phosphate *O*-acyltransferase 3		1.85		
	AB025408	Esterase 10		1.89		
	AF080580	Coq7		2.62		
	X68378	Cathepsin d		2.01		
	AW125874	Asparaginyl-rRNA synthetase		2.58		
	AW122030	Similar to phosphoserine aminotransferase		9.00		
	AW210370	Glucan (1,4-α-), branching enzyme 1	1.85	2.43		
	AI574278	Insulin-degrading enzyme		2.11		
	AW045202	Similar to disulfide isomerase-related protein		2.71		
	AI649453	Cytoplasmic tRNA synthetases	1.44	2.45		
	AW120896	Deoxyribonuclease H α	2.45		3.94	
	AI840339	Ribonuclease, RNase A family 4			1.54	
	AI196896	Fibrinogen β			1.28	
	Z23077	*S*-adenosylmethionine decarboxylase	1.95			
	L09737	GTP cyclohydrolase 1	1.46			
	AF071068	Aromatic-*L*-amino-acid decarboxylase	1.99			
	AF020039	NADP-dependent isocitrate dehydrogenase	1.39			
	AF071068	Dopa decarboxylase	1.99			
	AI851321	Uridindiphosphoglucosepyrophosphorylase 2	1.35			
	AW125336	Pyruvate dehydrogenase β	1.23			
	AI117848	Similar to mannosyl (α-1,6-)-Glycoprotein β-1,2-*N*-acetylglucosaminyltransferase	2.06			
	AI194855	Tryptophan 2,3-dioxygenase	1.25			
	AI840013	Δ2-enoyl-coenzyme A isomerase			1.72	
Kinase/phosphatase	AJ238636	Nucleoside diphosphatase	2.39	3.89		1.57
	AI845584	Dual specificity phosphatase 6	2.43			
Cell growth	AW049795	Transforming growth factor β-regulated gene 1		2.57		
	U35142	Retinoblastoma-binding protein mRbAp46		1.92		
	AF084524	Cellular repressor of EIA-stimulated genes	2.03	3.25	1.58	
	M60523	Idb3	1.61			
	AI326963	Angiopoietin-like 4			1.52	
Apoptosis	AF061972	Tat-interacting protein TIP30		3.03		
	AF041054	EIB 19K/Bcl-2-binding protein homolog		1.79		1.55
	US1052	Defender against Apoptotic Death (Dad1) gene		1.83		
	AI837599	Neural stem cell derived survival protein precursor		2.31		
	AV373612	Bag3	2.45			
	AA260005	Pawr			1.56	
Signal transduction	U06834	Eph receptor B4		2.91		
Signal regulating molecule	X56831	Mannose-6-phosphate-receptor		2.04		
	AW123904	GABA receptor-associated protein-like 1	1.31			
	AF023482	HSI-associating protein		1.82		
	AF069542	NFκB essential modulator		2.46		
	AF020185	Protein inhibitor of nitric-oxide synthase, light chain 1		2.13		
	AW121185	Protein inhibitor of nitric-oxide synthase, heavy chain 1		1.85		
	AF100694	Pontin52		3.89		
	L32751	Ran		2.71		
	D86563	Rab 4	1.37	2.27		
	U37413	Gna11, guanine nucleotide-binding protein		2.23		
	D29802	p205, G protein β subuit-like		1.79		
	AF115480	cAMP-dependent Rap1 Guanine-nucleotide exchange factor	2.22		2.19	
	AV349152	Regulator of *G*-protein signaling 16			2.28	
	Y00884	Cai, calcium-binding protein		4.23		
	D87898	ARF1		2.01		
	AJ222586	Precursor NEFA protein		6.15		
Cellular communication	M81445	Connexin	1.44		1.39	
Protease inhibitor	X69832	Serine proteinase inhibitor 2,4	2.97	7.57		
	M64086	Spi2 proteinase inhibitor		3.29		

TABLE I—*continued*

Categories of genes	Accession no.	Description of genes	AFC (D3T/vehicle)			
			WT[a]			*nrf2-keap1*[b] *double KO*
			6 h	*24 h*	*Diet (7 days)*	*24 h*
Transcription factor	M94087	mATF4	1.66			
Nuclear receptor and regulators	AW123880	X-box binding protein 1		2.08		
	AB012276	ATF7		3.61		
	U70736	COP9 subunit 5		2.23		
	AF009328	mCAR2 (Nuclear receptor subfamily 1)		2.69		2.45
	J03297	Tumor rejection antigen gp96		5.54		
Zinc finger proteins	AF062071	Zinc finger protein ZNF216	2.23			
mRNA processing	AJ839477	Poly(rC)-binding protein 1		1.97		
	L15447	Small nuclear RNA		1.92		
	AI183202	Heterogeneous nuclear ribonucleoprotein A1	3.73			
	U14648	Splicing factor, arginine/serine-rich 10	1.55			
Protein synthesis	U76112	Translation repressor NAT1		2.03		
	AB003502	Guanine nucleotide regulatory protein-1		1.96		
	X15267	Acidic ribosomal phosphoprotein PO		1.74		
	M25149	Tissue-specific transplantation antigen P91A		2.43		
	AW061243	eIF2a		1.83		
	U70733	eIF3-p44		1.89		
	U67328	Translation initiator factor3s8		1.99		
	M11408	16 S ribosomal protein		1.69		
	AI839717	Ribosomal protein L18		1.79		
Protein trafficking	AF096868	Vesicle-docking protein, 115kD		2.43		
	AI843665	Sec23a		1.79		
	AI848343	Sec23b	1.67			
	AB032902	Sec61		1.8		
	AB025218	Intracellular protein transport		2.28		
	U10119	Vacuolar protein sorting 4b	1.34			
	AI849207	Golgi reassembly stacking protein 2	1.29			
	AF029982	SERCA2	4.17			
Cancer-related	AJ845538	Etv6 (TEL oncogene)		5.82		
	J04596	GRO1 oncogene			4.99	
	AI839363	Mammary tumor integration site 6		1.93		
	Z31362	Neoplastic progression 3	4.79	32.22		
	L29441	Tumor differentially expressed 1		2.27		
	U22516	Angiogenin precursor		2.53		
Cytoskeletal	L20509	Matricin		2.64		
Organization/binding proteins	M21495	Actin, gamma		2.17		
	AW050256	Tubulin, β 3	2.01			
	X04663	Tubulin, β 5	1.87			
	J04953	Gelsolin	2.53			
	D37837	L-fimbrin	1.64			
	AW122536	Profilin 2		6.45		
	AB025406	Sid23		1.88		
	M22479	α tropomyosin		2.35		
	L00919	Protein 4.1		2.83		
Transport	D87990	UDP-galactose transporter-related isozyme 1		2.71		
	AW123952	Na^+/K-transporting, α 1 polypeptide		1.85		
	AA833514	ATP-binding cassette C3		2.62		1.44
	AW123338	FXYD domain-containing ion transport regulator		1.85		
	M73696	Solute carrier family 20, member 1	1.96			
	AW121716	Syntaxin 5a	1.97			
Lipid-related genes	M64248	Apolipoprotein A-IV		3.34		
	AI785422	Apolipoprotein A-V	1.25			
Immunity proteins	AF070975	Amyloid β (A4) precursor protein-binding A3		2.27		
	M23552	Serum amyloid P-component		2.07		
	U60438	Serum amyloid A protein isoform 2		5.86		
	M17790	Serum amyloid A		5.58		
	M25149	Tissue-specific transplantation antigen P91A		2.43		
	M35525	Hemolytic complement		4.03		
	X07698	CD8b	1.50	3.36		
	AI843732	Histocompatibility 13		1.84		
	AI853542	Small inducible cytokine A19	1.36			
	AW125865	Histocompatibility 47	1.66			
	A1790328	1K cytokine	1.74			
	M90551	ICAM-1			3.73	
	L12029	SDF-1-α			1.51	
	A1790328	JK cytokine			1.67	
	AV374868	Cytokine inducible SII2-containing protein 3			4.69	
Nuclear proteins	D49733	Lamin A		2.93		
	AA866971	Nucleolar protein GU2		2.13		
Cell adhesion	AW123694	Glycoprotein 110	2.41			
	AA760613	Lectin		2.10		

Nrf2-dependent, D3T-inducible Genes in keap1-nrf2 Double Knockout Mice—Gene expression profiles were examined in the liver of *keap1-nrf2* double knockout mice to determine whether loss of Keap1, the putative sensor target for D3T, altered inducer-mediated gene expression patterns beyond that affected by loss of Nrf2. Overall, 94% of genes induced by D3T in

TABLE I—*continued*

Categories of genes	Accession no.	Description of genes	AFC (D3T/vehicle)			
			WT[a]			*nrf2-keap1*[b] *double KO*
			6 h	*24 h*	*Diet (7 days)*	*24 h*
Other	M17551	Carbon catabolite repression 4 homolog		2.77	1.43	
	AA656775	Regulator for ribosome resistance homolog		2.04		
	AA529583	MORF-related gene X		2.79		
	AI846849	Mrps18b		2.48		
	M10062	Intracisternal A particles		2.04		
	L22977	X-linked lymphocyte-regulated 3b		2.48		
	U73039	Next to the Brca1		1.80		1.35
	X16672	Gag protein		1.77		
	X61453	NCK-associated protein 1		1.99		
	AI849838	Cullin 1		1.59		
	AW122453	Cysteine and histidine-rich domain (CHORD)-Containing, zinc-binding protein 1		1.93		
	D87973	Impact	3.23			
	AI255961	Hepeidin antimicrobial peptide	2.36			
	AF063095	Sel1b	1.77			
	AI551087	Intracisternal A particles			1.71	
	X80508	YAP65			1.39	

[a] Genes induced by D3T in wild type mice only, but not in *nrf2*-disrupted mice following single administration (6 h and 24 h) or administration in diet for 7 days compared to vehicle-treated wild-type mice.

[b] Genes induced by D3T in *keap1-nrf2* double knockout mice 24 h after treatment compared to vehicle-treated double knockout mice. Listed genes exhibited CV < 1 and appeared in at least seven of nine comparisons as described in "Experimental Procedures." No value indicates no effect on gene expression under these criteria.

wild-type mice were not increased in *keap1-nrf2* double knockout mice. Among the 231 genes classified as Nrf2-dependent, D3T-inducible from the wild-type to *nrf2*-disrupted comparisons, just 15 genes including *Cyp4a14*, *Cyp2c39*, *mEH*, and *GST* theta2 were increased in these double knockout mice (Table I). Since the *keap1-nrf2* double knockout mice behave like *nrf2* single knockout mice upon D3T treatment, it appears that most D3T-inducible genes are induced through the Keap1-Nrf2 complex.

Nrf2-dependent, D3T-repressed Genes—Shown in Table II, D3T treatment repressed the expression of 31 genes at 24 h and 30 largely overlapping genes following dietary administration of D3T in a Nrf2-dependent manner. Several cytochrome P450 isozymes (Cyp4a12, Cyp2d9, Cyp7a1, and Cyp8b1) were repressed by D3T treatment although no phase 2 genes were so affected. Expression levels of carbonic anhydrase 3 and 14 were reduced by half. An intriguing category of genes repressed by D3T treatment was the cholesterol/lipid biosynthesis metabolism-related genes. The transcription factor, sterol regulatory element-binding protein-1, which regulates cholesterol and lipid biosynthesis, was repressed 50–70% in the single gavage and dietary treatment groups.

RT-PCR Confirmation of Microarray Results—Induction and repression of genes by D3T treatment and the effects of *nrf2* genotype on the microarray results were confirmed using RT-PCR analysis in the 24-h treatment group (Fig. 2*A*). Gene-specific PCR primers were designed and RT-PCR reactions carried out. Gel images were quantified using densitometry and normalized using amplified albumin gene intensities. Expression levels of 22 genes among the D3T-inducible genes were analyzed by RT-PCR. NQO1 transcript levels were increased 10-fold by D3T in wild-type mice compared with vehicle-treated counterparts and were not increased in *nrf2*-disrupted mice in the RT-PCR analysis. Microarray analysis had indicated that NQO1 was increased 6-fold by D3T in the wild-type mice only. Transcripts levels for mEH, GST Mu3, and Hsp40 homolog showed 4.6-, 3.7-, and 5.5-fold increases, respectively, by D3T treatment in wild-type mice according to RT-PCR analysis. Corresponding fold changes of these genes in the microarray analysis were 4.0, 4.6, and 4.1, respectively. Expression of proteasome subunits were also confirmed and showed comparable induction by RT-PCR analysis. Representative repressed genes (sterol regulatory element-binding protein-1 and carbonic anhydrase 3) detected in the microarray analysis also showed reduced mRNA levels by RT-PCR analysis.

RT-PCR analysis was also performed to confirm the results from the microarray analysis in the double knockout mice (Fig. 2*B*). Expression levels of NQO1, GST Mu3, p58, proteasome subunits beta type 3 and 26 S proteasome-associated pad1 homolog were not increased by D3T treatment in the liver of *keap1-nrf2* double knockout mice, while, mEH was slightly increased.

DISCUSSION

Nrf2 is a critical transcription factor for mediating amplification of the mammalian defense system against environmental stresses. To identify the genes regulated by Nrf2, global gene expression patterns were examined in mouse liver following D3T treatment of *nrf2* single and *keap1-nrf2* double knockout mice using oligonucleotide microarray analysis. For evaluation of the microarray data, altered gene expression levels having a CV of less than 1 and significant differences in at least 7 of 9 possible comparisons were selected so as to filter out false positive responses. Filtering out false positive genes enabled the detection of induced genes with average fold changes of 1.2 and greater and of repressed genes under 0.7. The fold changes confirmed by RT-PCR consistently reflected the average fold changes observed in the microarray analyses. For example, induction of genes showing less than 2-fold increases by microarray analysis (*eIF3p-44* and *Sec61*) exhibited similar fold changes by RT-PCR analysis. These results indicate that filtering genes by considering reproducibility and biological variance in individual responses provided an effective means to identify genes affected to small, but potentially biologically important degrees.

Genes increased or decreased by D3T treatment in wild-type but not *nrf2*-disrupted animals were classified as Nrf2-dependent genes. While, some genes increased in both genotypes, they showed higher fold induction in wild-type mice compared with *nrf2*-disrupted mice. These included heat shock protein 86 kDa 1 ($AFC_{D3T}/AFC_{Vehicle}$; 4.11/1.39), *Cyp2a4* (37.01/2.16), *Cyp3a13* (3.41/1.73), UDP-glucose dehydrogenase (24 h after treatment, 7.52/1.67), and lipocalin (15.46/2.87). Therefore, expression of

TABLE II
Hepatic Keap1-Nrf2 complex-dependent, D3T-repressed genes

Categories of genes	Accession no.	Description of genes	AFC (D3T/vehicle)		
			WT[a]		*nrf2-keap1*[b] *double KO*
			24 h	*Diet (7 days)*	*24 h*
Stress response genes	J04633	Hsp90		0.61	
Xenobiotic-metabolizing enzymes	Y10221	Cyp4a12	0.6		
	M27168	Cyp2d9		0.75	
	L23754	Cyp7a1		0.46	
	AF090317	Cyp8b1		0.54	
General enzymes	M15268	Aminocvulinic acid synthase 2, erythroid	0.45	0.62	
	M27695	Urate oxidase	0.42		
	AJ006474	Carbonic anhydrase 111	0.08	0.50	
	AB005450	Carbonic anhydrase 14		0.56	
	M88694	Thioether *S*-methyltransferase	0.43	0.54	
	AI840501	Camello-like 1	0.42		
	AI790931	Fructose-1,6-bisphosphatase	0.61		
	M27347	Clastase 1, pancreatic	0.41		
	AI506285	Coagulation factor X	0.60		
Cell growth	M31680	Growth hormone receptor	0.39		
	U15012	Growth hormone receptor	0.60	0.62	
Signal transduction/ signal regulating molecules	AF089751	ATP receptor P2X4 subunit	0.68		
	AI834950	Similar to nuclear receptor subfamily 1, group D	0.59		
	M80631	G protein α subunit	0.17		
Transcription factor	AI843895	Sterol regulatory element binding factor 1	0.29	0.43	0.44
Cancer-related	AI845538	Etv6 (TEL oncogene)		0.41	
Growth arrest	M21828	Growth arrest specific 2	0.34		
Cytoskeletal proteins binding proteins	X99921	S100 calcium-binding protein A13	0.61	0.62	
	M16465	S100a 10 calcium binding protein A11		0.64	
Immunity proteins	U47737	Lymphocyte antigen 6 complex, defense response	0.45		0.69
Lipid/steroid-related	M64248	Apolipoprotein A-IV		0.61	
	M75886	Hydroxysteroid dehydrogenase 2	0.28		
	M77015	3-β-hydroxysteroid dehydrogenase		0.46	
	Y14660	Fatty acid binding protein L-FABP	0.46		
	X58426	Lipoprotein lipase	0.56		
	AI838021	Fatty acid coenzyme A ligase, long chain 5	0.46		
	X95279	Spot14	0.14	0.41	
	AI848668	Sterol-C4-methyl oxidase-like	0.55		
	AF057368	Δ7-sterol reductase	0.31		
Transport	AF045692	Solute carrier family 16, member 2	0.59		
	D00073	Transthyretin	0.33		
	X70533	Corticosteroid binding globulin	0.36		
Others	U07425	Heparin cofactor 11 precursor	0.54		

[a] Genes repressed by D3T in wild type mice only, but not in *nrf2*-disrupted mice following single administration (24 h) or administration in diet for 7 days compared to vehicle-treated wild-type mice.
[b] Genes repressed by D3T in *keap1-nrf2* double knockout mice 24 h after treatment compared to Vehicle-treated double knockout mice. Listed genes exhibited CV < 1 and appeared in at least seven of nine comparisons as described in "Experimental Procedures". No value indicates no effect on gene expression under these criteria.

these genes by D3T treatment was affected by the *nrf2*-genotype. Collectively, there were 231 Nrf2-dependent, D3T-induced genes detected 24 h after treatment, representing 79% of total D3T-induced genes in wild-type mice. Similar percentages of Nrf2-dependent genes among all D3T-induced genes were observed at 6 h after a single treatment and with dietary exposure to D3T for 1 week. Thus, the large majority of D3T-induced genes appeared to be regulated through the Nrf2 pathway in mouse liver; 50% of D3T-repressed genes were also Nrf2-dependent genes.

The products of genes induced by D3T through a Nrf2-dependent pathway can be classified as xenobiotic metabolizing enzymes, antioxidants, general enzymes, chaperone/stress response proteins, ubiquitin/proteasome systems, protein trafficking proteins, acute response/immunity proteins, cytoskeletal organization proteins, membrane transport proteins, signaling molecules, transcription-related genes, and RNA processing and translation-related factors. This profile of changes in gene expression evoked by D3T is similar to that of the cellular response to oxidative stress in mammalian cells (36). The gene categories most affected by *nrf2* genotype were xenobiotic metabolizing genes, antioxidants and proteasome subunits. D3T treatment induced genes belonging to other categories such as cytoskeletal organization proteins, and acute response genes in *nrf2*-disrupted mice; however, very few xenobiotic metabolizing genes and proteasome subunits were induced in the *nrf2*-knockout mice. These Nrf2-specific inducible gene categories may be critical contributors to the cytoprotective and chemopreventive effects of dithiolethiones.

Induction of xenobiotic detoxifying genes and antioxidants by dithiolethiones in a Nrf2-dependent manner is consistent with our previous results. Seven isozymes of GST and glutathione-related genes (glutathione reductase and γ-glutamylcysteine ligases) were induced as expected and expression levels of *NQO1*, *mEH*, and UDP-glucuronyl transferase 2 family, member 5 were increased by D3T only in wild-type mice. Novel xenobiotic-metabolizing genes regulated by Nrf2 pathway are carbonyl reductase, flavin-containing monooxygenase 1, aldo-keto reductase 1A1, and aldehyde oxidase. Induction of carbonyl reductase, aldo-keto reductase 1A1, and aldehyde oxidase may contribute to the protective effects of dithiolethiones by detoxifying cytotoxic reactive carbonyl compounds (37–39). Induction of the antioxidant genes, peroxiredoxin, thioredoxin reductase, and thioredoxin restore normal cellular redox status under situations of oxidative stress (40). Other reducing pathways, namely, NADPH-generating enzymes such as UDP-glu-

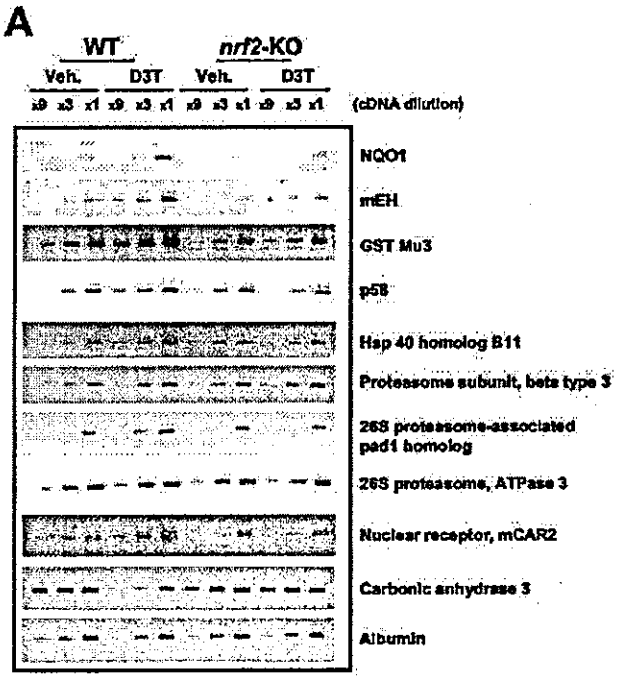

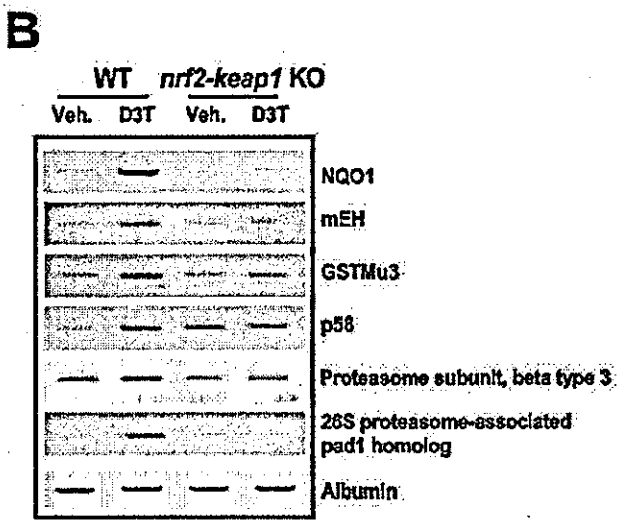

FIG. 2. **RT-PCR analyses.** *A*, RT-PCR analysis of Nrf2-dependent, D3T-inducible genes in mouse liver. Gene-specific PCR primers were used to detect mRNA levels of each gene. PCR amplification was carried out with serially diluted cDNAs from vehicle (*Veh.*) or D3T-treated wild-type (*WT*) and *nrf2*-knockout mice (*nrf2*-KO). Albumin levels were used for normalization. *B*, RT-PCR analyses for NQO1, mEH, GST Mu3, p58, proteasome subunit beta type 3, and 26 S proteasome-associated pad1 homolog were performed with cDNA from vehicle (*Veh.*) or D3T-treated wild-type (*WT*) and *keap1-nrf2* double knockout mice (*keap1-nrf2* KO).

cose dehydrogenase and malate oxidoreductase were increased by D3T, again in an Nrf2-dependent pathway.

A previously unrecognized category of Nrf2-dependent, D3T-inducible genes is the ubiquitin/proteasome system. Twenty-six genes from this system were elevated by D3T treatment in wild-type mice. As depicted in Fig. 3, the genechip used in this study contains 39 genes related to proteasomes, and 67% of these proteasome genes were significantly induced by D3T. A substantial shift in the distribution of expression ratios was seen in this class of genes relative to all of the genes on the array ($p < 0.001$). By comparison, the expression distribution of

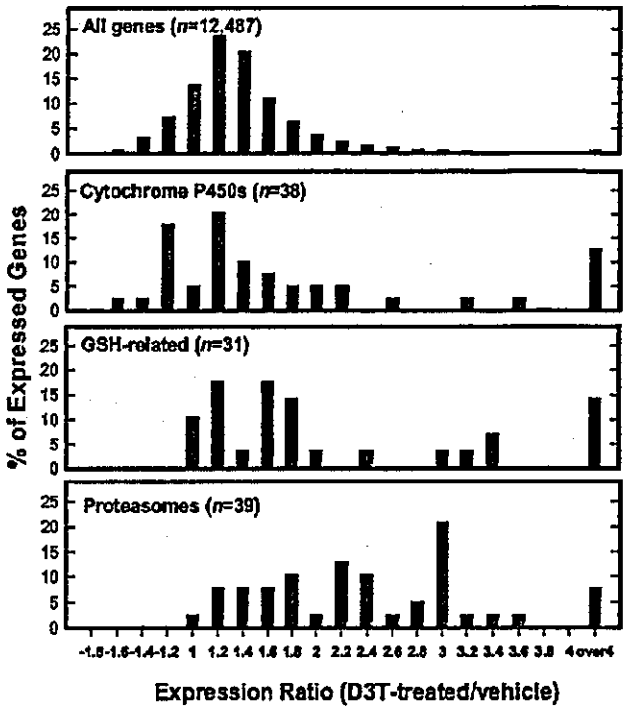

FIG. 3. **Distribution profiles of genes as a function of their expression ratios.** Ratios are those for D3T-treated over vehicle-treated wild-type mice. The distributions are for total genes (n = 12,487), cytochrome P450s (n = 38), glutathione (GSH)-related genes (n = 31), and proteasomes (n = 39). The numbers indicate the number of genes in each functional category contained on the mouse genechip. The distribution of D3T-induced proteasome genes is significantly different from the distribution for total genes ($p < 0.001$, Mann-Whitney rank sum test).

glutathione synthetic and utilizing genes, reflecting a large number of known Nrf2-ARE regulated genes, was trimodal whereas that of 38 cytochrome P450 genes indicated an overall lack of responsiveness of these genes to D3T. A small subset of highly inducible P450s is apparent, however. Among the induced 26 S proteasome subunits, six subunits showed induction in both genotypes; however, induced fold changes were considerably higher in wild-type mice than *nrf2*-knockout mice. D3T treatment also induced heat shock proteins. These chaperone proteins together with the ubiquitin/proteasome system play an essential role in response to stress (41, 42). Accumulation of unfolded polypeptides following oxidative stress can disturb normal cellular functions and trigger apoptosis through the JNK pathway (42, 43). Heat shock proteins including Hsp40, Hsp70, Hsp90, and small Hsp (α-cystallin and Hsp27) function as molecular chaperones, and bind selectively to denatured or partially unfolded polypeptides (44). Many studies indicate that accumulation of unfolded or misfolded proteins induces a response in which chaperone genes and components of the ubiquitin pathway are up-regulated to repair damaged proteins in mammalian cells (45, 46). These induced heat shock proteins serve protective roles in neurons and expression of Hsp70 and Hsp40 protected neuronal cells from apoptosis by abnormal protein accumulation (47, 48). Increased expression of 26 S proteasome subunits by oxidative stress has not been reported in mammalian systems, although, proteasome subunits can be induced by interferon-γ in human cell lines during viral infection (49). The expression of 26 S proteasome subunits is coordinately regulated by the transcription factor Rpn4p in *Saccharomyces cerevisiae*, and their expression can be affected by stress (50, 51). However, there does not appear to be any

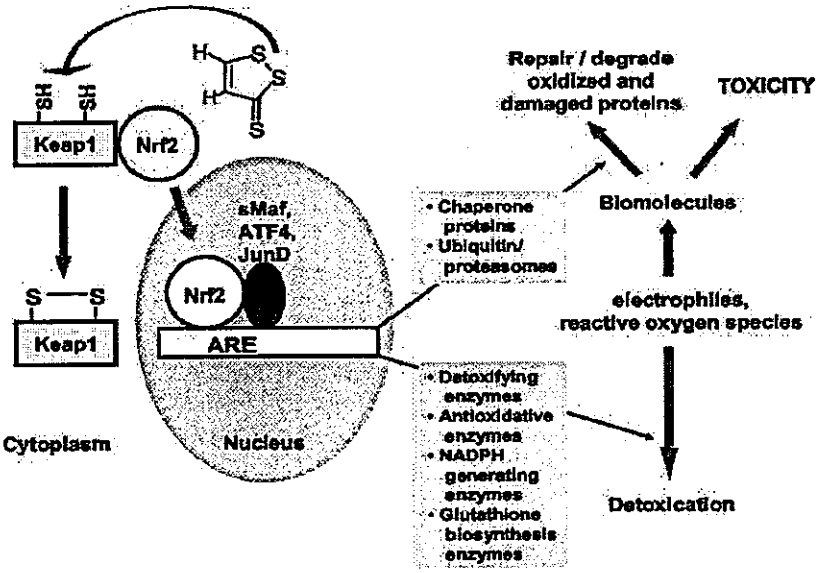

FIG. 4. A model for Keap1-Nrf2 complex dependent genes involved in cytoprotection against environmental stresses. Dithiolethiones may react with sulfhydryl groups of Keap1 and liberate Nrf2 to translocate into the nucleus. Nrf2 transactivates the ARE with other bZIP proteins to increase the expression of detoxifying and antioxidative enzymes, NADPH-generating enzymes, glutathione biosynthesis enzymes, chaperone proteins, and ubiquitin-proteasomes. These gene products promote protection against electrophiles and reactive oxygen species from environmental and endogenous sources by detoxifying these reactive intermediates and enhancing the repair and degradation of damaged proteins.

homology between Rpn4p and Nrf2. The increased expression of proteasome subunits by D3T in the presence of Nrf2 indicates that Nrf2 may be a common transcriptional regulator for the expression of 26 S proteasomes upon stress conditions in mammalian cells. Recently, Sekhar *et al.* (52) have shown that Nrf2 is degraded by the ubiquitin-proteasome pathway and that Nrf2 can be co-immunoprecipitated with ubiquitin polymer. Induction of chaperone and proteasome genes by D3T may facilitate the repair or degradation of damaged or oxidized proteins as an additional means to respond to oxidative and electrophilic stresses (Fig. 4).

Gene expression patterns were studied at different times. Many xenobiotic metabolizing genes were increased rapidly and persistently following a single dose of D3T, while genes related to restoration of damaged biomolecules such as the ubiquitination-proteasome system were principally elevated at 24 h. General enzymes, protein trafficking proteins and cytoskeletal components were increased early and only transiently after treatment. Relatively few gene transcripts remained elevated after feeding a D3T-containing diet for 7 days. The phase 2 detoxifying genes and proteasomes, with the exception of mEH, did not maintain their elevated transcript levels during continuous dietary exposure to D3T. These results indicate that repetitive administration of an Nrf2 activator may induce a cellular adaptation to the continuous signaling of gene transcription. This refractory transcriptional response to repetitive administration of dithiolethiones is consistent with our earlier observations (53). Comparison of the levels of GST subunit proteins and catalytic activity, mRNA levels and transcriptional rates of *gst a1* showed that transcript level and transcription rate returned to near basal levels after 3 days of feeding the dithiolethione oltipraz, while, protein levels and activity remained maximally elevated for at least 1 week with feeding. Presumably altered post-translational modifications to the induced proteins contribute to the sustained GST activity. Thimmulappa *et al.* (19) has shown Nrf2-dependent, sulforaphane-inducible genes in the small intestine of mice following 7 daily doses of sulforaphane by gavage. They identified 26 genes as Nrf2-dependent, sulforaphane-inducible genes, and this gene cluster included xenobiotic-metabolizing enzymes, glutathione biosynthesis enzymes, and NADPH-generating enzymes. Whereas, these results are in accord with our present findings, they indicate that dosing schedule and sampling time influence the dynamics of gene expression. Therefore, analysis of gene expression patterns 24 h after single administration of inducer appears optimal for identifying Keap1Nrf2-dependent pathways. Companion proteomic analyses, however, are likely to reveal additional contributors to inducible cytoprotective responses.

The cytoplasmic repressor of Nrf2, Keap1 has been proposed to be a cellular sensor for protection against oxidative and electrophilic stresses. Direct interaction of enzyme inducers with cysteine residues of Keap1 has been demonstrated recently using the irreversible sulfhydryl reactant dexamethasone mesylate (16). Several cysteines in the intervening region of Keap1 are modified by this inducer. The chemical basis of dithiolethione activation of Nrf2 signaling is not clear as yet; however, dithiolethiones are sulfhydryl reactive compounds (54, 55) and stimulate the translocation of Nrf2 into the nucleus (8, 11). The critical role of Keap1 in the regulation of Nrf2 function has been established in studies using *keap1*-knockout mice. *keap1*-disrupted mice are not viable after 3 weeks of age; however, expression levels of phase 2 detoxifying genes such as GST and NQO1 are much higher in neonatal *keap1*-disrupted animals than in age-matched wild-type mice (33). The lethal phenotype of the *keap1*-disrupted mouse can be rescued by conjoint disruption of Nrf2 expression. Gene expression profiles in *keap1-nrf2* double knockout mice following D3T treatment clearly show that most D3T-inducible genes are under the control of the Keap1-Nrf2 complex. Most (94%) of genes induced by D3T in wild-type mice were not increased in these double knockout mice. Fifteen genes classified as Nrf2-dependent, D3T-induced genes in the wild-type to *nrf2*-disrupted mice comparisons were induced in these *keap1-nrf2* double knockout mice. These genes included mEH and GST theta 2, suggesting a partial recovery of alternative regulatory pathway(s) to express these protective genes in the double knockout mice.

The Keap1-Nrf2 complex appears to be the primary molecular target of chemopreventive agents such as the dithiolethiones. D3T increases the expression of a broad range of genes in a Keap1-Nrf2-dependent manner that act to directly detoxify toxins as well as generate essential cofactors such as glutathione and reducing equivalents. Induction of genes involved in the recognition and repair of damaged proteins expands the role of *nrf2*-dependent genes beyond primary control of electrophilic and oxidative stresses into secondary protective actions.

Because dithiolethiones lose protective efficacy in *nrf2*-disrupted mice, these D3T-inducible, Keap1-Nrf2-dependent genes are likely to be central contributors to cell survival.

Acknowledgments—We thank Kim Mai of the Microarray Core of the NIEHS Center in Urban Environmental Health for assistance with the microarray analyses. We also thank Patrick Dolan for maintaining and genotyping mice.

REFERENCES

1. Kensler, T. W. (1997) *Environ. Health Perspect.* **105**, 965–970
2. Hayes, J. D., and McMahon, M. (2000) *Cancer Lett.* **174**, 103–113
3. Wang, J. S., Shen, X., He, X., Zhu, Y. R., Zhang, B. C., Wang, J. B., Qian, G. S., Kuang, S. Y., Zarba, A., Egner, P. A., Jacobson, L. P., Munoz, A., Helzlsouer, K. J., Groopman, J. D., and Kensler, T. W. (1999) *J. Natl. Cancer Inst.* **91**, 347–354
4. Lam, S., MacAulay, C., Le Riche. J. C., Dyachkova, Y., Coldman, A., Guillaud, M., Hawk, E., Christen, M. O., and Gazdar, A. F. (2002) *J. Natl. Cancer Inst.* **94**, 1001–1009
5. Rushmore, T. H., King, R. G., Paulson, K. E., and Pickett, C. B. (1990) *Proc. Natl. Acad. Sci. U. S. A.* **87**, 3826–3830
6. Favreau, L., and Pickett, C. B. (1995) *J. Biol. Chem.* **270**, 24468–24474
7. Moinova, H. R., and Mulcahy, R. T. (1998) *J. Biol. Chem.* **273**, 14683–14689
8. Kwak, M-K., Itoh, K., Yamamoto, M., and Kensler, T. W. (2002) *Mol. Cell. Biol.* **22**, 2883–2892
9. Venugopal, R., and Jaiswal, A. K. (1996) *Proc. Natl. Acad. Sci. U. S. A.* **93**, 14960–14965
10. Itoh, K., Chiba, T., Takahashi, S., Ishii, T., Igarashi, K., Katoh, Y., Oyake, T., Hayashi, N., Satoh, K., Iatayama, I., Yamamoto, M., and Nabeshima, Y. (1997) *Biochem. Biophys. Res. Commun.* **236**, 313–322
11. Kwak, M-K., Itoh, K., Yamamoto, M., Sutter, T. R., and Kensler, T. W. (2001) *Mol. Med.* **7**, 135–145
12. Itoh, K., Wakabayashi, N., Katoh, Y., Ishii, T., Igarashi, K., Engel, J. D., and Yamamoto, M. (1999) *Genes Dev.* **13**, 76–86
13. Dhakshinamoorthy, S., and Jaiswal, A. K. (2001) *Oncogene* **20**, 3906–3917
14. Zipper, L. M., and Mulcahy, R. T. (2002) *J. Biol. Chem.* **277**, 36544–36552
15. Sekhar, K. R., Spitz, D. R., Harris, S., Nguyen, T. T., Meredith, M. J., Holt, J. T., Guis, D., Marnett, L. J., Summar, M. L., and Freeman, M. L. (2002) *Free Radic. Biol. Med.* **32**, 650–662
16. Dinkova-Kostova, A. T., Holtzclaw, W. D., Cole, R. N., Itoh, K., Wakabayashi, N., Katoh, Y., Yamamoto, M., and Talalay, P. (2002) *Proc. Natl. Acad. Sci. U. S. A.* **99**, 11908–11913
17. MacMahon, M., Itoh, K., Yamamoto, M., Chanas, S. A., Henderson, C. J., McLellan, L. I., Wolf, C. R., Cavin, C., and Hayes, J. D. (2001) *Cancer Res.* **61**, 3299–3307
18. Primiano, T., Gastel, J. A., Kensler, T. W., and Sutter, T. R. (1996) *Carcinogenesis* **17**, 2297–2303
19. Thimmulappa, R. K., Mai, K. H., Srisuma, S., Kensler, T. W., Yamamoto, M., and Biswal, S. (2002) *Cancer Res.* **62**, 5196–5203
20. Lee, J. M., Hanson, J. M., Chu, W. A., and Johnson, J. A. (2001) *J. Biol. Chem.* **276**, 20011–20016
21. Enomoto, A., Itoh, K., Nagayoshi, E., Haruta, J., Kimura, T., O'Conner, T., Harada, T., and Yamamoto, M. (2001) *Toxicol. Sci.* **59**, 169–177
22. Chan, K., and Kan, Y. W. (1999) *Proc. Natl. Acad. Sci. U. S. A.* **96**, 12731–12736
23. Chan, K., Han, X. D., and Kan, Y. W. (2001) *Proc. Natl. Acad. Sci. U. S. A.* **98**, 4611–4616
24. Cho, H-Y., Jedlicka, A. E., Sekhar, M. S., Reddy, P. M., Zhang, L. Y., Kensler, T. W., Yamamoto, M., and Kleeberger, S. R. (2001) *Am. J. Respir. Cell Mol. Biol.* **26**, 42–51
25. Kwak, M-K., Egner, P. A., Dolan, P. M., Ramos-Gomez, M., Groopman, J. D., Itoh, K., Yamamoto, M., and Kensler, T. W. (2001) *Mutat. Res.* **480–481**, 305–315
26. Aoki, Y., Sato, H., Nishimura, N., Takahashi, S., Itoh, K., and Yamamoto, M. (2001) *Toxicol. Appl. Pharmacol.* **173**, 154–160
27. Ramos-Gomez, M., Dolan, P. M., Itoh, K., Yamamoto, M., Talalay, P., and Kensler, T. W. (2003) *Carcinogenesis*, in press
28. Ramos-Gomez, M., Kwak, M-K., Dolan, P. M., Itoh, K., Yamamoto, M., Talalay, P., and Kensler, T. W. (2001) *Proc. Natl. Acad. Sci. U. S. A.* **98**, 3410–3415
29. Wattenberg, L. W., and Bueding, E. (1986) *Carcinogenesis* **7**, 1379–1388
30. Rao, C. V., Rivenson, A., Katiwalla, M., Kelloff, G. J., and Reddy, B. S. (1993) *Cancer Res.* **53**, 2502–2506
31. Kensler, T. W., Egner, P. A., Dolan, P., Groopman, J. D., and Roebuck, B. D. (1987) *Cancer Res.* **47**, 4271–4277
32. Kensler, T. W., Groopman, J. D., Eaton, D. L., Curphey, T. J., and Roebuck, B. D. (1992) *Carcinogenesis* **13**, 95–100
33. Yamamoto, M., Wakabayashi, N., Iahii, T., Kobayashi, M., Kato, Y., and Itoh, K. (2002) *Proceedings of the 14th International Symposium on Microsomes and Drug Oxidation*, p. 48, Sapporo, Japan
34. Li, J., and Johnson, J. A. (2002) *Physiol. Genomics* **9**, 137–144
35. Bouton, C. M., and Pevsner, J. (2002) *Bioinformatics* **18**, 323–324
36. Halliwell, B., and Gutteridge, J. M. C. (1999) *Free Radicals in Biology and Medicine*, Oxford University Press, Inc., New York
37. Forrest, G. L., and Gonzalez, B. (2000) *Chem. Biol. Interact.* **129**, 21–40
38. Oppermann, U. C., and Maser, E. (2000) *Toxicology* **144**, 71–81
39. Yoshihara, S., and Ohta, S. (1998) *Arch. Biochem. Biophys.* **360**, 93–98
40. Tanaka, T., Nakamura, H., Nishiyama, A., Hosoi, F., Masutani, H., Wada, H., and Yodoi, J. (2000) *Free Radic. Res.* **33**, 851–855
41. Gabai, V. L., Meriin, A. B., Yaglom, J. A., Volloch, V. Z., and Sherman, M. Y. (1998) *FEBS Lett.* **438**, 1–4
42. Gabai, V., L., Meriin, A. B., Mosser, D. D., Caron, A. W., Rits, S., Shifrin, V. I., and Sherman, M. Y. (1997) *J. Biol. Chem.* **272**, 18033–18037
43. Samali, A., and Orrenius, S. (1998) *Cell Stress. Chaperones* **3**, 228–236
44. Johnson, J. L., and Craig, E. A. (1997) *Cell* **90**, 201–204
45. Watt, R., and Piper, P. W. (1997) *Mol. General Genet.* **253**, 439–447
46. Hershko, A., and Ciechanover, A. (1998) *Annu. Rev. Biochem.* **67**, 425–479
47. Kobayashi, Y., Kume, A., Li, M., Doyu, M., Hata, M., Ohtsuka, K., and Sobue, G. (2000) *J. Biol. Chem.* **275**, 8772–8778
48. Satyal, S. H., Schmidt, E., Kitagawa, K., Sondheimer, N., Lindquist, S., Kramer, J. M., and Morimoto, R. I. (2000) *Proc. Natl. Acad. Sci. U. S. A.* **97**, 5750–5755
49. Foss, G. S., Larsen, F., Solheim, J., and Prydz, H. (1998) *Biochim. Biophys. Acta* **1402**, 17–28
50. Xie, Y., and Varshavsky, A. (2001) *Proc. Natl. Acad. Sci. U. S. A.* **98**, 3056–3061
51. Ng, D. T., Spear, E. D., and Walter, P. (2000) *J. Cell Biol.* **150**, 77–88
52. Sekhar, K. R., Yan, X. X., and Freeman, M. L. (2002) *Oncogene* **21**, 6829–6834
53. Davidson, N. E., Egner, P. A., and Kensler, T. W. (1990) *Cancer Res.* **50**, 2251–2255
54. Levron, B., Burgot, G., and Burgot, J. L. (2000) *Arch. Biochem. Biophys.* **382**, 189–194
55. Carey, K. A., Kensler, T. W., and Fishbein, J. C. (2001) *Chem. Res. Toxicol.* **14**, 939–945

Keap1 regulates both cytoplasmic-nuclear shuttling and degradation of Nrf2 in response to electrophiles

Ken Itoh[1,2], Nobunao Wakabayashi[2], Yasutake Katoh[1,2], Tetsuro Ishii[2], Tania O'Connor[2] and Masayuki Yamamoto[1,2,*]

[1]*Exploratory Research for Advanced Technology, Japan Science and Technology Corporation, and* [2]*Center for Tsukuba Advanced Research Alliance and Institute of Basic Medical Sciences, University of Tsukuba, 1-1-1 Tennoudai, Tsukuba 305-8577, Japan*

Abstract

***Background*: Transcription factor Nrf2 regulates the expression of a set of detoxifying and anti-oxidant enzyme genes. Several lines of evidence suggest that electrophiles and reactive oxygen species liberate Nrf2 from its cytoplasmic repressor Keap1 and provoke the accumulation of Nrf2 in the nucleus. To elucidate the molecular mechanisms as to how Nrf2 is activated by inducers, we examined the cytoplasmic-nuclear shuttling and turnover of Nrf2.**

***Results*: We found that Nrf2 is rapidly degraded through the proteasome pathway, while electrophiles cause Nrf2 nuclear translocation with concomitant stabilization. Crucial to the inducible accumulation of Nrf2 is the enfeebling of the Nrf2–Keap1 interaction by electrophiles. Exploiting mice which have the *LacZ* reporter gene knocked into the *nrf2* locus, we revealed that the inducible accumulation of Nrf2 protein by electrophiles in macrophages and intestinal epithelia could be recapitulated by the Nrf2 N-terminal region in combination with a nuclear localization signal. We also found constitutive Nrf2 nuclear accumulation in Keap1-deficient mouse macrophages.**

***Conclusions*: Our results highlight the fact that Nrf2 protein turnover is regulated by Keap1 mediated subcellular compartmentalization.**

Introduction

To counteract the damage that can be provoked by electrophiles and reactive oxygen species (ROS), higher animals have developed elaborate defence mechanisms (Prestera *et al.* 1993; Primiano *et al.* 1997). A battery of genes encoding detoxifying and anti-oxidative stress enzymes/proteins is coordinately induced following exposure to electrophiles and ROS (Beutler *et al.* 1995; Hayes & Pulford 1995). This coordinated response is regulated through a *cis*-acting element called the anti-oxidant responsive element (ARE) or electrophile responsive element (EpRE) within the regulatory region of target genes (Rushmore *et al.* 1991; Friling *et al.* 1990). Genes encoding a subset of drug metabolizing enzymes, such as glutathione S-transferases (GSTs) (Friling *et al.* 1990) and NAD(P)H-quinone oxidoreductase 1 (NQO1) (Rushmore *et al.* 1991), have been shown to be under ARE/EpRE regulation, along with a subset of anti-oxidant genes, such as haem oxygenase-1 (HO-1) (Alam *et al.* 1995), the subunits of γ-glutamylcysteine synthetase (γ-GCS) (Mulcahy *et al.* 1997) and thioredoxin (Kim *et al.* 2001).

Nrf2/ECH (NF-E2-Related Factor 2 (Moi *et al.* 1994) or chicken Erythroid-derived CNC-Homology factor (Itoh *et al.* 1995)) was recently identified as the major regulator of ARE-mediated gene expression (reviewed in Itoh *et al.* 1999b; Ishii *et al.* 2002). Nrf2/ECH belongs to the Cap-N-Collar (CNC) family of transcription factors that share a highly conserved basic region-leucine zipper (bZip) structure (reviewed in Motohashi *et al.* 1997). Nrf2 requires a member of the small Maf proteins as an obligatory partner molecule for binding to their cognate DNA sequence (Itoh *et al.* 1995; Marini *et al.* 1997). Through *nrf2* gene targeting analysis, we demonstrated that Nrf2 regulates a battery of genes encoding drug metabolizing enzymes and anti-oxidant proteins (Itoh *et al.* 1997; Ishii *et al.* 2000). Subsequently, we identified Keap1 (Kelch-like ECH

Communicated by: Shunsuke Ishii
**Correspondence*: E-mail: masi@tara.tsukuba.ac.jp

Associating Protein 1) as a direct binding partner of Nrf2 (Itoh *et al.* 1999a). The central role attributed to the Nrf2-Keap1 system is the regulation of cellular defence against a variety of environmental insults; for example, in the electrophile counterattack response (Itoh *et al.* 1999b; Ishii *et al.* 2000), in acetaminophen intoxication (Enomoto *et al.* 2001), in chemical carcinogenesis (Ramos-Gomez *et al.* 2001), and in diesel exhaust inhalation (Aoki *et al.* 2001).

Several key features have emerged from an extensive study of the molecular mechanisms of Nrf2 activation by electrophiles and ROS. In peritoneal macrophages, nuclear Nrf2 accumulation in response to electrophiles or ROS appears to be an important step in Nrf2 mediated gene induction (Ishii *et al.* 2000). Forced over-expression of Nrf2 gave rise to ARE-reporter gene transcription in a reporter co-transfection/transactivation assay (Itoh *et al.* 1999a) and switched on endogenous target genes in zebrafish (Kobayashi *et al.* 2002) without any additional electrophilic or oxidative signals. Therefore, increasing the amount of Nrf2 circumvents the normal activation pathway of electrophiles and ROS and actuates cytoprotective gene transcription. In the co-transfection/transactivation model, the concomitant expression of Keap1 sequesters Nrf2 in the cytoplasm and represses Nrf2 transactivation activity (Itoh *et al.* 1999a). Treatment of the cells with electrophiles liberates Nrf2 from Keap1. Nrf2 subsequently translocates to the nucleus and activates the transcription of cytoprotective enzyme genes through the ARE.

While these results clearly demonstrate that electrophiles or ROS induce a subset of cytoprotective enzyme genes by counteracting Keap1 repression of Nrf2 activity, many questions still remain regarding the manner by which electrophilic signals dissociate Nrf2 from Keap1, and Nrf2 translocates from the cytoplasm to the nucleus. To address these questions, we investigated the accumulation, stability and nuclear-cytoplasmic shuttling of Nrf2 in mouse peritoneal macrophages. Our results indicate a rapid turnover of Nrf2 in the cytoplasm under non-stress conditions, whereas Nrf2 protein stabilizes in the presence of electrophiles and accumulates in the nucleus. We found that the N-terminal region of Nrf2, in combination with the Nuclear Localization Signal (NLS), is sufficient for this electrophilic induced nuclear accumulation, and that Keap1 plays important roles in this process by interacting with the Nrf2 N-terminal Neh2 domain. Our data suggest that the N-terminal region of Nrf2 initiates rapid proteolysis within the cytoplasm, but mediates turnover via a slower pathway in the nucleus.

Results

Electrophiles accumulate Nrf2 protein in peritoneal macrophages

To elucidate the molecular basis of the Nrf2 activation mechanism in response to electrophiles, we examined the relationship between Nrf2 activation and Nrf2 target gene induction in primary cultures of peritoneal macrophages. We executed a time course study of Nrf2 target gene induction (Fig. 1A) and Nrf2 accumulation in the nucleus (Fig. 1B) using diethylmaleate (DEM), an electrophile classified as a Michael reaction acceptor. The inducible expression of Peroxiredoxin I (*Prx*I)/MSP23, one of the major Nrf2 target genes in peritoneal macrophages (Ishii *et al.* 2000), occurred as early as 2 h after DEM treatment (Fig. 1A, top panel). In contrast, the mRNA level of Nrf2 was slightly reduced by DEM treatment (Figs 1A and 2A, middle panels), indicating that DEM was inducing the expression of the Nrf2 target gene through some post-transcriptional mechanism.

The Nrf2 protein level in the nuclear fraction was examined by immunoblot analysis using anti-Nrf2 antibody. Nrf2 migrated as 110 kDa in SDS-PAGE, which was the same as over-expressed recombinant Nrf2 in 293T cells (Fig. 1C, lane 8; Kwak *et al.* 2002). A significant increase in Nrf2 was observed as early as 0.5 h following DEM treatment (Fig. 1B). We also found that Nrf2 binding activity to the ARE sequence was markedly increased and showed a similar induction profile (data not shown). This is consistent with our previous analysis in that, although Nrf2 target genes are significantly induced, Nrf2 mRNA is not increased after the treatment of macrophages with DEM or similar agents (Ishii *et al.* 2000). These results demonstrate that the nuclear accumulation of Nrf2 precedes induction of target gene expression and is thus a key event in the inducible expression of phase II and anti-oxidant enzyme genes.

We then examined whether Nrf2 accumulation can be detected in total cell lysate (Fig. 1C). Importantly, before DEM treatment, Nrf2 was scarcely detectable in total cell lysate, indicating that the size of the cytoplasmic Nrf2 pool is very small in non-induced cells. Following DEM treatment, however, Nrf2 accumulated in total cell lysate, albeit the immunoblot signal was very weak compared to that with nuclear extracts. Electrophiles other than DEM, such as menadione (lane 2), chlorodinitrobenzene (CDNB) (lane 4), and sulforaphane (lane 5) provoked a similar accumulation of Nrf2 in total cell lysate (Fig. 1D), showing that cellular Nrf2 accumulation is a mechanism which is common to several Nrf2 inducers.

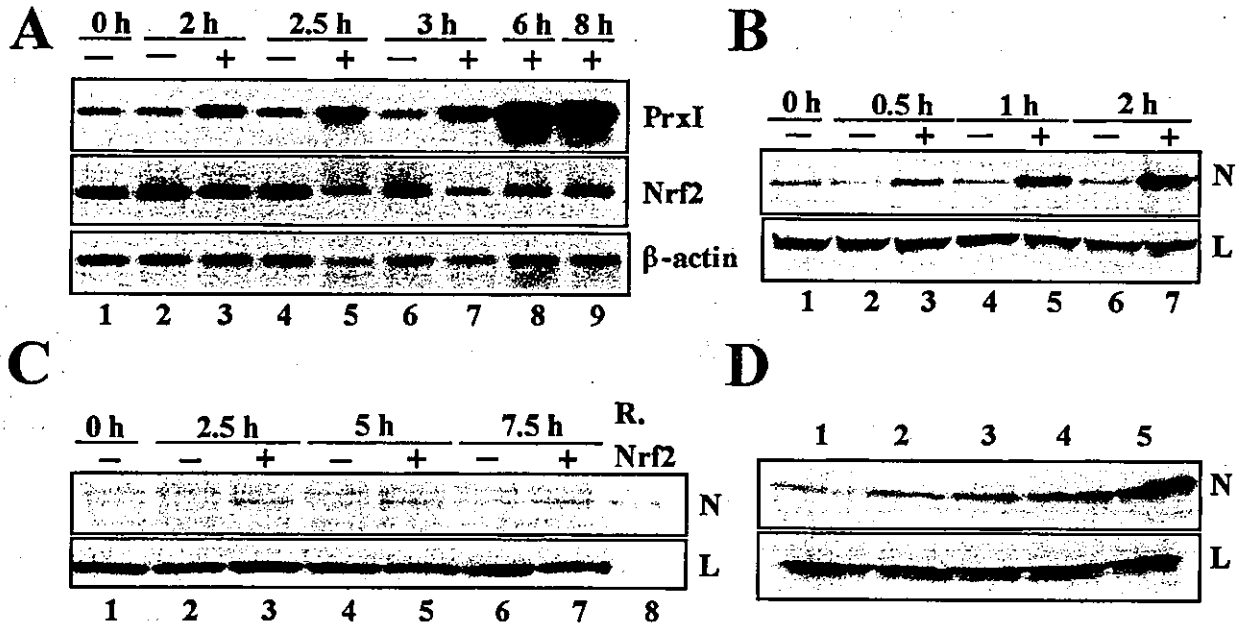

Figure 1 Nrf2 activation by DEM accompanies the accumulation of Nrf2 in whole cell lysates. (A) RNA blot analysis of Nrf2 and *Prx*I. Peritoneal macrophages were cultured in the presence (lanes 3, 5 and 7–9) or absence of 100 μM DEM (lanes 1, 2, 4 and 6), and total RNAs were prepared at the various time points indicated in the Figure. (B) DEM caused Nrf2 to accumulate in the nucleus. Nuclear extracts from macrophages treated with (lanes 3, 5 and 7) or without (lanes 1, 2, 4 and 6) 100 μM DEM for the indicated times were immunoblotted with either anti-Nrf2 antibody (N) or anti-Lamin B antibody (L). (C) Nrf2 accumulated in total cell extracts after treatment with DEM. Total cell extracts from macrophages treated with (lanes 3, 5 and 7) or without (lanes 1, 2, 4 and 6) 100 μM DEM for the indicated times were immunoblotted with either anti-Nrf2 antibody (N) or anti-Lamin B antibody (L). Over-expressed recombinant Nrf2 in 293T cells (R. Nrf2) was also loaded as a control (lane 8). (D) Nrf2 was accumulated in total cell lysates by various electrophiles and ROS producing agents. Total cell extracts prepared from macrophages treated with DMSO (lane 1), 2.5 μM menadione (lane 2), 100 μM DEM (lane 3), 10 μM CDNB (lane 4), or 10 μM sulforaphane (lane 5) for 4 h were immunoblotted with anti-Nrf2 antibody (N) or anti-Lamin B antibody (L).

Since the Nrf2 protein signal was scarcely detectable in immunoblot analysis of the cytosolic fraction (data not shown), we assume that Nrf2 accumulation in the nucleus mainly occurs through new protein synthesis and not through the translocation of pre-existing Nrf2 protein from the cytosol to the nucleus.

De novo protein synthesis is required for nuclear accumulation of Nrf2

In order to test whether *de novo* protein synthesis is required for nuclear accumulation of Nrf2, we treated peritoneal macrophages with DEM in either the presence or absence of the protein synthesis inhibitor cycloheximide (CHX). The induction of *Prx*I mRNA by DEM was largely abolished in the presence of CHX (1 μg/mL; Fig. 2A). Similarly, the induction of HO-1 mRNA by DEM was significantly affected by CHX treatment (data not shown). The major regulator of inducible defence gene expression may therefore have a short degradation half-life and rapid turnover.

Since Nrf2 mRNA levels did not significantly increase following treatment by DEM and/or CHX, the possibility exists that Nrf2 protein actually turns over rapidly and its level decreases in response to CHX, hence giving rise to the decrease in Nrf2 target gene expression. We therefore examined the effect of CHX on the levels of nuclear Nrf2. The build up of Nrf2 in the 0.5% Triton X insoluble nuclear fraction can be monitored biochemically (Fig. 2B). Nrf2 accumulated in the Triton X insoluble fraction, but not in the soluble fraction, of peritoneal macrophages from control, DEM-treated and DEM plus CHX-treated mice. Although DEM markedly induced the Nrf2 level (compare lanes 2 and 4), CHX largely cancelled this induction (lane 6). These results thus indicate that Nrf2 turns over rapidly in macrophages and that new protein synthesis is required for the nuclear accumulation of Nrf2.

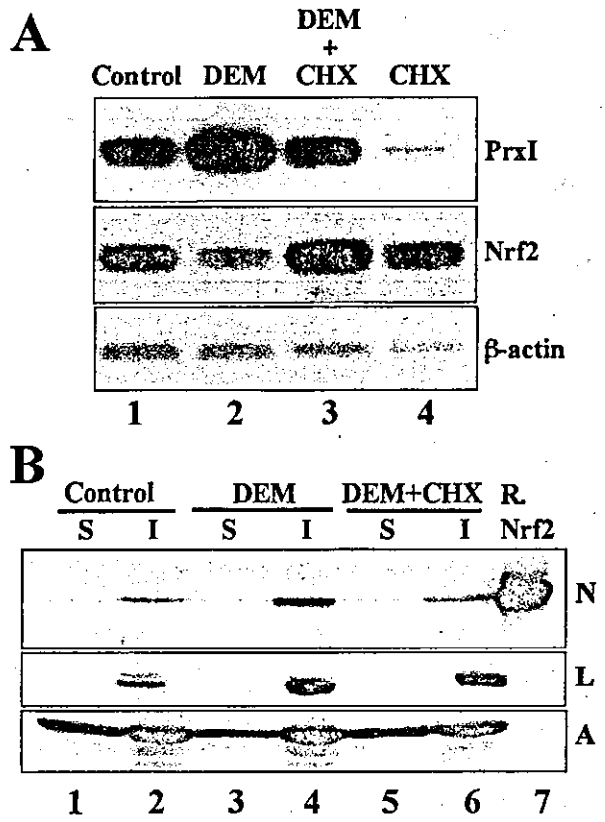

Figure 2 Both the induction of target genes and the activation of Nrf2 are sensitive to treatment with cycloheximide (CHX). (A) The effect of CHX on the induction of *Prx*I. Total RNAs prepared from macrophages that were untreated (lanes 1) or treated with either 100 μM DEM (lane 2), 1 μg/mL CHX (lane 4) or both (lane 3) for 4.5 h were blot hybridized with the cDNA probes indicated in the figure. (B) Macrophages were either untreated (lanes 1 and 2) or treated with 100 μM DEM (lanes 3 and 4) or both DEM and CHX (lanes 5 and 6) for 4 h and 0.5% Triton X soluble (S) (lanes 1, 3 and 5) or insoluble (I) (lanes 2, 4 and 6) fractions were prepared. Fractions were probed with anti-Nrf2 antibody (N), anti-lamin B antibody (L), or anti-β-actin antibody (A). Over-expressed recombinant Nrf2 in 293T cells (R, Nrf2) was also loaded as a control (lane 7).

Proteasome inhibitors also induce Nrf2 accumulation

In order to gain insight into the rapid turnover rate of Nrf2, we carried out two further experiments. Firstly, we examined the effect of various protease inhibitors on the level of Nrf2 protein. Immunoblot analysis using Nrf2 antibody revealed that proteasome inhibitors, such as clasto-Lactacystin β-Lactone, MG132 and MG115, led to the accumulation of Nrf2 in the Triton X insoluble fraction, but that a calpain inhibitor failed to accumulate Nrf2 (Fig. 3A, top panel). Our results suggest the degradation of Nrf2 specifically by the proteasome system in non-induced cells.

Second, we analysed the effect of electrophiles on Nrf2 protein turnover. Since the expression level of Nrf2 in the total cell lysate of peritoneal macrophages was too low to measure quantitatively, we induced the intracellular level of Nrf2 protein by MG132, a reversible inhibitor of proteasome, for 2.5 h (Lee & Goldberg 1998). After the thorough removal of MG132 and treatment of the peritoneal macrophages with CHX and/or DEM, the Nrf2 protein level in the total cell lysate was measured by immunoblot analysis with anti-Nrf2 antibody. Nrf2 was rapidly degraded with a half-life of 18.5 min, whereas DEM stabilized the Nrf2 protein and prolonged its intracellular half-life to 31.7 min (Fig. 3B,C). To clarify the mechanism of Nrf2 stabilization by DEM, we examined the effect of DEM in the presence of a saturating amount of MG132. If DEM had worked through a different pathway than MG132 to accumulate Nrf2, they should synergistically accumulate Nrf2. As shown in Fig. 3D, DEM did not affect the protein level of Nrf2, suggesting that DEM attenuates the pathway leading to the proteasomal degradation of Nrf2. From this, we postulate that Nrf2 protein is stabilized by electrophiles through the inhibition of proteasomal Nrf2 degradation.

The N-terminus of Nrf2 and the NLS are sufficient for the electrophilic response

We generated a germ line *nrf2* mutant mouse by replacing exon V of the *nrf2* gene, which encodes the DNA binding and dimerization domains, with an NLS-LacZ-neo (nuclear localization signal-*LacZ*-neomycin resistant gene) cassette (Itoh *et al.* 1997). This genetically engineered mouse expressed the *Nrf2-LacZ* fusion gene, giving rise to a protein product containing the N-terminal portion of Nrf2 and complete β-galactosidase. The structure of the fusion protein is shown in Fig. 4A. However, although we are confident that the knock-in targeting was executed in a flawless manner, it puzzled us that we could not detect β-galactosidase activity or its protein in these mutant mice. This was particularly strange since mRNA encoding the Nrf2-LacZ fusion protein was expressed at a level comparable to endogenous Nrf2 mRNA (Itoh *et al.* 1997). The finding that Nrf2 is rapidly degraded *in vivo* prompted us to examine whether the β-galactosidase protein might also be rendered unstable due to its fusion with the N-terminal region of Nrf2.

To test the effect of MG132 and DEM on the level of Nrf2-lacZ protein, we carried out several series of

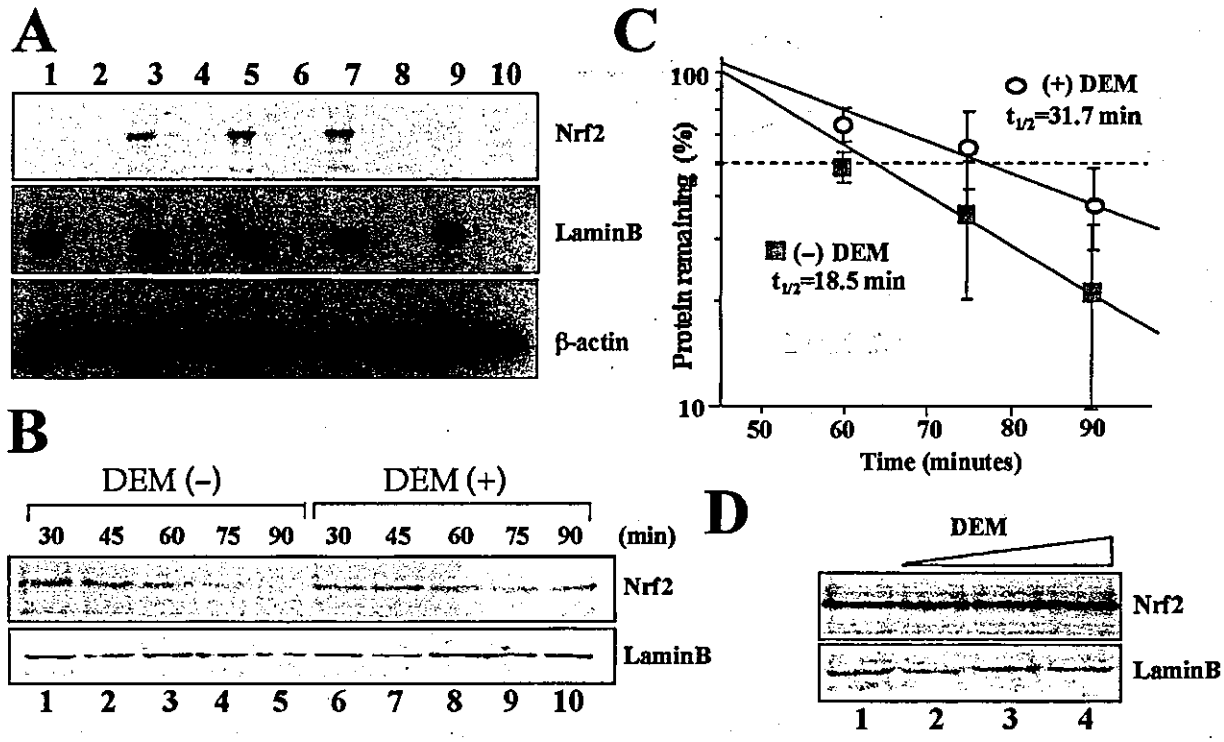

Figure 3 DEM inhibits the degradation of Nrf2 by proteasomes. (A) Nrf2 protein was accumulated in the 0.5% Triton X insoluble fraction by specific proteasome inhibitors. Macrophages were treated with DMSO (lanes 1 and 2), 10 μM MG132 (lanes 3 and 4), 10 μM clasto-Lactacystin β-Lactone (lanes 5 and 6), 50 μM MG115 (lanes 7 and 8), or 10 μM calpain inhibitor (lanes 9 and 10) for 4.5 h. The 0.5% Triton soluble (lanes 2, 4, 6, 8 and 10) or insoluble (lanes 1, 3, 5, 7 and 9) fractions were prepared and immunoblotted with the indicated antibody. (B) Total cell lysates from macrophages treated with 1 μg/mL CHX in the presence or absence of 100 μM DEM for the indicated times were subjected to immunoblot analysis with anti-Nrf2 antibody or anti-Lamin B antibody. (C) The band intensities in (B) were measured by densitometric analysis. The relative Nrf2 band intensities (Nrf2/Lamin B) are shown against a semilog plot. (D) The cells were treated with 10 μM MG132 alone (lane 1) or in combination with 50 (lane 2), 100 (lane 3) or 200 μM (lane 4) DEM for 4 h. Total cell lysates were subjected to immunoblot analysis with anti-Nrf2 antibody or anti-Lamin B antibody.

experiments exploiting the homozygous *Nrf2-LacZ* knock-in mouse (we will refer to this mouse as *nrf2*$^{-/-}$) and peritoneal macrophages derived from this mouse. We first determined the Nrf2-LacZ protein level in peritoneal macrophages from the *nrf2*$^{-/-}$ mouse treated with either MG132 or DEM using anti-LacZ and anti-Nrf2 antibodies. Showing very good agreement with our previous analysis, the Nrf2-LacZ protein was not detectable in peritoneal macrophages in primary culture (Fig. 4B, lane 1). In contrast, accumulation of Nrf2-LacZ protein, which migrates to approximately the 180 kDa-size position, was clearly identified in the macrophages treated with either DEM (lane 2) or MG132 (lane 3) by both anti-LacZ antibody (Fig. 4B) and anti-Nrf2 antibody that specifically recognizes the N-terminal region of Nrf2 (data not shown). These results thus revealed that the N-terminus of Nrf2 is responsible for the accumulation of Nrf2 in response to DEM.

We previously found that Nrf2 is essential for the BHA induction of phase II drug metabolizing enzymes and anti-oxidant stress enzymes/proteins in the intestine and liver (Itoh *et al.* 1997; Ishii *et al.* 2000). Based on this, we next examined the effect of BHA on the level of Nrf2-LacZ protein *in vivo*. After feeding the *nrf2*$^{-/-}$ mice with BHA for 3 days, they were dissected and tissue sections of the intestine were examined immunohistochemically with anti-LacZ antibody. Consistent with our expectation, positive nuclear staining was observed specifically in the intestinal epithelium of BHA-treated *nrf2*$^{-/-}$ mice (Fig. 4C), but not in the sections of *nrf2*$^{-/-}$ mice fed on a normal diet (Fig. 4D). Thus, Nrf2-LacZ protein also turns over rapidly *in vivo*, with DEM and BHA preventing rapid degradation of the protein. Importantly, the *in vivo* level of Nrf2-LacZ mRNA remained constant during BHA induction (Fig. 4E). In conclusion, the N-terminus of Nrf2, in combination

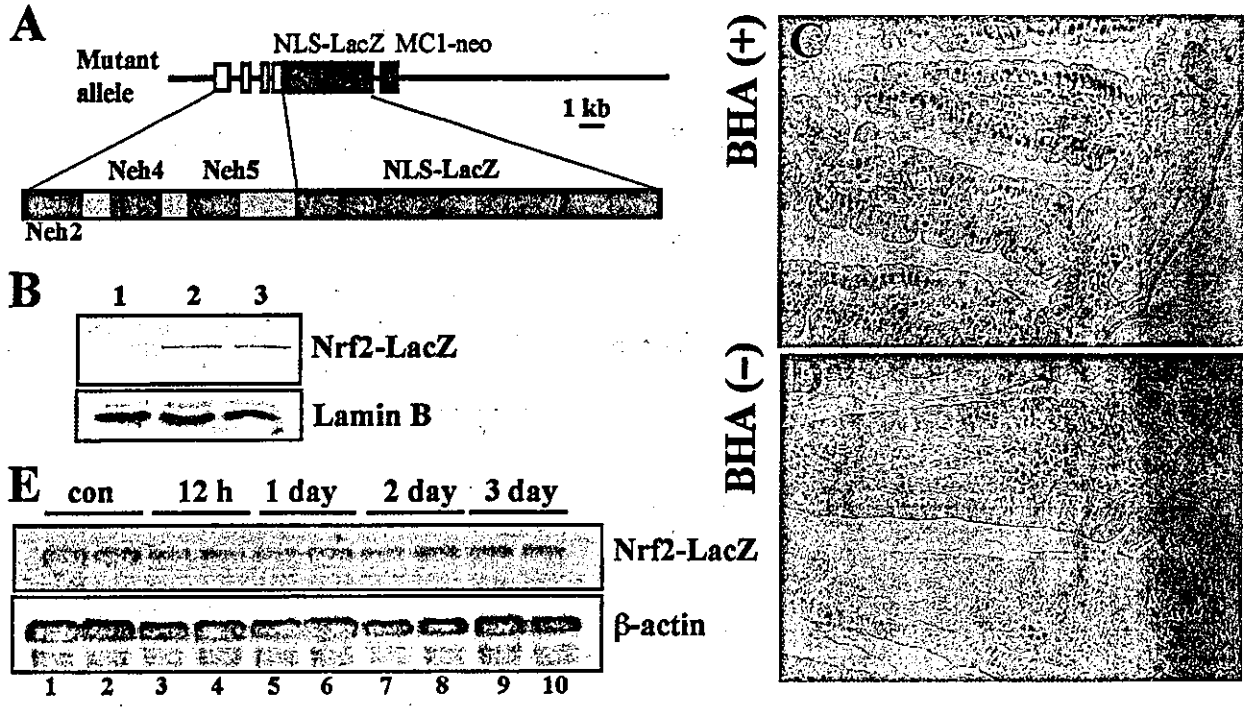

Figure 4 The N-terminal region of Nrf2 is sufficient for the response to electrophiles. (A) Schematic representation of the Nrf2 knock-in strategy. NLS-LacZ was knocked into exon V of the *nrf2* gene locus (top panel). The lower structure represents the resultant fusion protein. (B) Effect of DEM and MG132 on the Nrf2 LacZ fusion proteins. *nrf2*$^{-/-}$ peritoneal macrophages were untreated (lane 1) or treated with 100 μM DEM (lane 2) or 10 μM MG132 (lane 3) for 4 h and total cell lysates were subjected to immunoblot analysis using anti-LacZ antibody. (C) and (D) Immunohistochemical staining of BHA treated or untreated mice by anti-LacZ antibody. *nrf2*$^{-/-}$ mice were fed on a diet supplemented with (C) or without (D) 0.7% BHA for 3 days, and their tissue sections were analysed by anti-lacZ antibody. (E) RNA blot analysis of Nrf2-LacZ. *nrf2*$^{-/-}$ mice were fed in duplicate with a BHA-containing diet for the indicated periods and total RNAs were analysed by Nrf2 cDNA probe or β-actin probe.

with the NLS, is sufficient for the response to the proteasome inhibitor MG132, the electrophile DEM, and the dietary anti-oxidant BHA.

The Neh2 domain mediates proteasomal degradation

To determine which portion of the Nrf2 N-terminal region is recognized by proteasome, the Neh2, Neh4 and Neh5 domains of Nrf2 were independently fused to enhanced green fluorescent protein (EGFP) (Fig. 5A) and transfected into NIH3T3 mouse fibroblasts. Neh4-EGFP was excluded from the analysis, as its expression, even in the presence of MG132, could not be detected. Neomycin-resistant cells were selected and multiple mass stable transformants were established for each construct. Cells were treated with MG132 for 9 h in order to amass the fusion proteins and EGFP. After thoroughly washing MG132 from the cells, the degradation half-life of each EGFP fusion protein was determined in the presence of the protein synthesis inhibitor CHX by following a procedure similar to that used for Fig. 3. Intriguingly, the Neh2-EGFP protein level declined rapidly after the addition of CHX, with a degradation half-life of 3 h, whereas the levels of EGFP alone and Neh5-EGFP remained high, even 10 h after CHX treatment (Fig. 5B,C). The rapid degradation of the Neh2 domain was proteasome dependent, because treatment with MG132 along with CHX inhibited Neh2 degradation (data not shown).

The accumulation or rapid degradation of EGFP and its fusion proteins was visualized by green fluorescence. Since EGFP, and the Neh2 and Neh5 EGFP fusion proteins did not retain a canonical NLS, they dispersed throughout the cells. The important finding here is that, although cells transfected with EGFP or Neh5-EGFP showed bright green fluorescence (Fig. 5D,F), those expressing Neh2-EGFP showed only marginal fluorescence (Fig. 5E), reflecting the rapid turnover and low accumulation level of the Neh2-EGFP fusion protein.

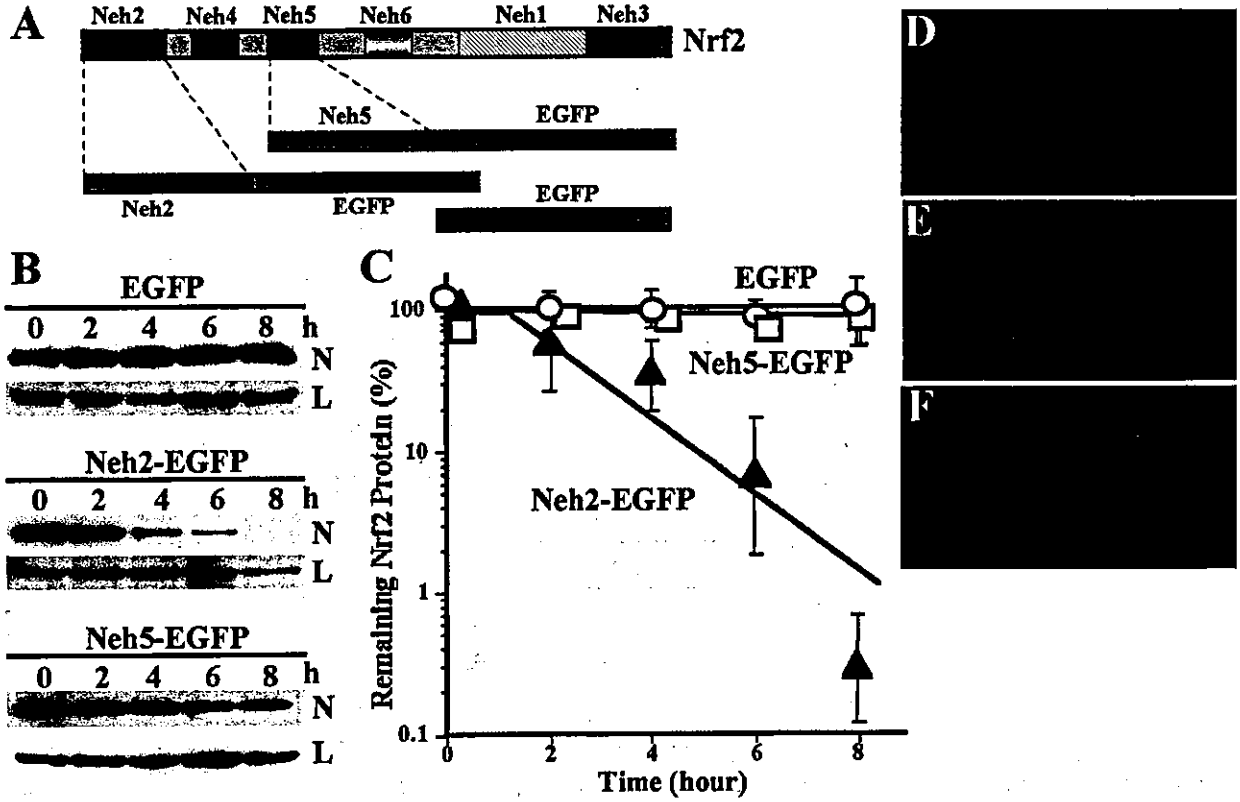

Figure 5 Neh2 mediates the rapid degradation of Nrf2. (A) Schematic representation of Nrf2-EGFP fusion proteins. 'Neh domain' stands for highly conserved regions of the Nrf2 protein within various species. Neh2 and Neh5 correspond to amino acid sequences 1–99 and 153–227, respectively. (B) Neh2 enhances the degradation of the reporter gene EGFP in the mouse fibroblast cell line NIH 3T3. Fusion proteins and EGFP were first accumulated by 10 μM MG132 for 9 h. The protein levels of EGFP (top panel), Neh2-EGFP (middle panel), or Neh5-EGFP (bottom panel) were determined using anti-EGFP antibody after treating the cells with 20 μg/mL CHX for the indicated times. (C) Determination of the degradation half-life of Neh2-EGFP. The band intensities in (B) were measured by densitometry. The relative EGFP values (EGFP/Lamin B) are shown against a semilog plot. (D–F) Localization of Nrf2-EGFP fusion proteins. NIH3T3 cells were transiently transfected with EGFP (D), Neh2-EGFP (E) or Neh5-EGFP (F).

Thus, these results clearly support our hypothesis that Neh2 is the core domain within the Nrf2 N-terminus which is responsible for mediating the rapid degradation of Nrf2.

The Nrf2 protein level was unaffected by electrophiles in Keap1-deficient peritoneal macrophages owing to its constitutive nuclear accumulation

Our revelation that Nrf2 is rapidly degraded by the proteasome system, and that such degradation requires the N-terminal region of Nrf2, led us to hypothesize that Keap1 may be an important regulator of Nrf2 stability *in vivo*. Therefore, we explored the roles of Keap1 in the process of Nrf2 degradation using mice constitutive for *keap1*, heterologous for *keap1*, or deficient in the *keap1* gene.

The juvenile death of *keap1* knockout mice due to squamous cell hyperkeratinization provoked by constitutive Nrf2 activation prevented us from obtaining sufficient peritoneal macrophages (manuscript submitted for publication). To circumvent this problem, we exploited *keap1*$^{-/-}$::*nrf2*$^{+/-}$ mice, which retain only one copy of the *Nrf2* gene and survive to the adult stage. Thus, the protein level of Nrf2 in peritoneal macrophages was examined against a genetic background of heterozygous *nrf2* in the presence of two, one or zero alleles of the *keap1* gene.

The basal level of Nrf2 protein was markedly higher in *keap1* knockout mouse peritoneal macrophages compared to those of *keap1* heterozygous mutant or wild-type mice (Fig. 6A, compare lanes 1, 4 and 7). It is important to note that the constitutive expression level of Nrf2 protein negatively correlated with the number of

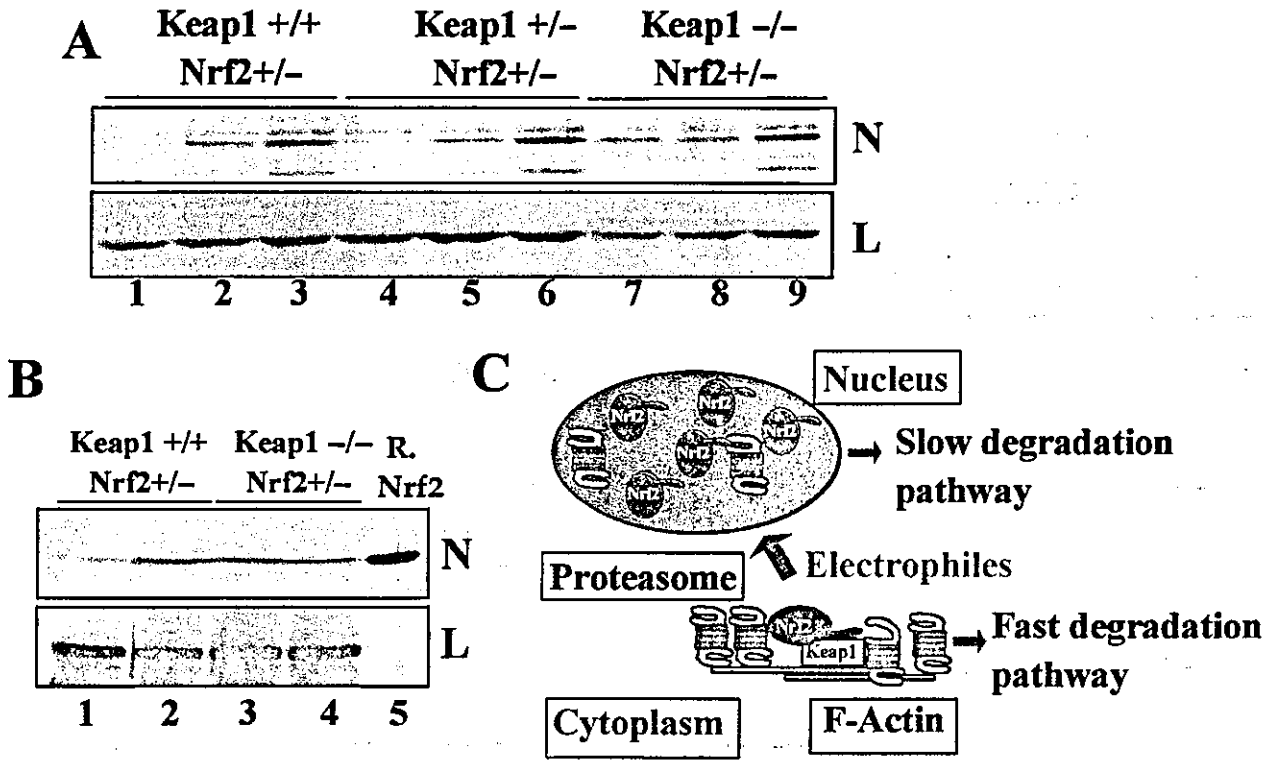

Figure 6 Nrf2 is constitutively accumulated in the nucleus and lacks the response to electrophiles in *keap1*$^{-/-}$ *nrf2*$^{+/-}$ peritoneal macrophages. (A) Nrf2 immunoblot analysis in *keap1* mutant macrophages. Peritoneal macrophages from wild-type (lanes 1–3), *keap1* heterozygous (lanes 4–6), and *keap1* homozygous (lanes 7–9) mice were either untreated (lanes 1, 4 and 7) or treated with 100 μM DEM (lanes 2, 5 and 8) or 10 μM MG132 (lanes 3, 6 and 9) for 3 h. Total cell extracts were subjected to immunoblot analysis using anti-Nrf2 antibody (upper panel). Anti-lamin B antibody was used as a loading control (lower panel). (B) Immunoblot analysis of nuclear extracts from *keap1*$^{-/-}$ macrophages. Macrophages from *keap1*$^{-/-}$ (lanes 3 and 4) or *keap1*$^{+/+}$ mice (lanes 1 and 2) were treated (lanes 2 and 4) or untreated (lanes 1 and 3) with 100 μM DEM for 3 h and nuclear extracts were subjected to immunoblot analysis using anti-Nrf2 antibody (upper panel). Anti-lamin B antibody was used as a loading control (lower panel). (C) Model of Nrf2 degradation. In the cytoplasm, Nrf2 is bound by Keap1 and subjected to rapid proteasomal degradation. Keap1 enhances proteasomal Nrf2 degradation by localizing Nrf2 near the proteasome. In the nucleus, Nrf2 is relatively stabilized by the lack of Keap1.

intact *keap1* alleles. The DEM mediated induction of Nrf2 was completely abolished in *keap1*$^{-/-}$ macrophages, because of the high constitutive expression of Nrf2 (lanes 2, 5 and 8). These results strongly support our contention that Keap1 sequestration to the cytosol enhances Nrf2 degradation. Based on these findings, we envisage that Keap1 maintains a minimal basal level of Nrf2 by directing the rapid degradation of Nrf2, thus allowing a sharp response to a sudden onslaught by electrophiles.

The addition of MG132 significantly increased the amount of Nrf2 protein (Fig. 6A, lanes 3, 6 and 9), even in *keap1*$^{-/-}$ macrophages where the level actually exceeded that brought about by DEM (compare lanes 8 and 9). This observation suggests that Nrf2 degradation in *keap1* (−/−) macrophages and DEM-treated macrophages is partially attenuated, with MG132 being the more specific inhibitor of the proteasomal degradation pathway. The examination of Nrf2 expression in the nucleus presented us with a clearer resolution of Nrf2 accumulation compared to that in total cells. The constitutive accumulation of Nrf2 was observed in nuclear extracts from Keap1-deficient macrophages (Fig. 6B, compare lanes 1 and 3), consistent with that observed in total cell extracts (Fig. 6A). This further suggested that Nrf2 was liberated from Keap1, hence the rapid degradation machinery, and efficiently accumulated in the nucleus. It should be noted that DEM elicited an increase in the nuclear Nrf2 level which was comparable to, but not greater than, the constitutive Nrf2 level in the Keap1 deficient animals (Fig. 6B, lanes 3 and 4), suggesting that DEM acts to increase the Nrf2 protein level by repressing Keap1 activity.

In summary, while the combination of Keap1 and proteasome rapidly turns over Nrf2 in non-induced